REVIEW

The thermodynamic design of heat and mass transfer processes and devices

Adrian Bejan*

This review article places in perspective the new work devoted both to the analysis of the thermodynamic irreversibility of heat and mass transfer components and systems and to the design of these devices on the basis of entropy generation minimization. The review focuses on the fundamental mechanisms responsible for the generation of entropy in heat and fluid flow and on the design tradeoff of balancing the heat transfer irreversibility against the fluid flow irreversibility. Applications are selected from the fields of heat exchanger design, thermal energy storage, and mass exchanger design. This article provides a comprehensive, up-to-date review of second-daw analyses published in the heat and mass transfer literature during the last decade.

Keywords: *second-law analysis, entropy generation minimization, exergy analysis*

Introduction

The objective of this review article is to outline the most basic steps of the procedure of entropy generation minimization (thermodynamic design) at the system-component level. This paper is a continuation of the review work attempted on two earlier occasions;[1,2] therefore, a further objective is to review the fundamental work published in this area in the 1980s.

The fundamental idea justifying the work of irreversibility minimization at the system-component level is that the overall entropy generation rate of the system is, in fact, the sum of the entropy generation contributions made by all the system's components. If the irreversibility of one component is minimized and the other components are untouched,† the irreversibility reduction registered at the component level shows up also at the overall system level.

The tradeoff between competing irreversibilities

The basic design problem is to determine the thermodynamically optimum size or operating regime of a certain engineering system, where by "optimum" we mean the condition in which the system destroys the least exergy while still performing its fundamental engineering function. It turns out that, in many systems, the various mechanisms and design features that account for irreversibility *compete* with one another. For this reason, the thermodynamic optimum that concerns us here is the condition of the most desirable tradeoff between two or more competing irreversibilities.

Internal flow and heat transfer

In view of the diversity of thermodynamic optimization problems—at least one problem of this type is contained in each power and refrigeration system design—we begin with some of the simplest illustrations of the basic design principle. Later, as we review the expanding literature of this field, we focus on more complex systems. Two simple elementary features (subcomponents) in the constitution of most power and refrigeration installations are the heat exchanger passage and the fin. Both features account for most of the heat exchanger. Consider first a heat exchanger passage, which is a duct of arbitrary cross section (A) and arbitrary wetted perimeter (p). The engineering function of the passage is specified in terms of the heat transfer rate per unit length (q') that is to be transmitted to the stream ($\dot{m}$); that is, both q' and $\dot{m}$ are specified. In the steady state, the heat transfer q' crosses the temperature gap ΔT formed between the wall temperature ($T+\Delta T$) and the bulk temperature of the stream (T). The stream flows with friction in the x direction; hence, the pressure gradient $(-dP/dx)>0$.

Taking as thermodynamic system a passage of length dx, the first law and the second law state

$$\dot{m}\,dh = q'\,dx \tag{1}$$

$$\dot{S}'_{\text{gen}} = \dot{m}\frac{ds}{dx} - \frac{q'}{T+\Delta T} \geq 0 \tag{2}$$

where $\dot{S}'_{\text{gen}}$ is the entropy generation rate per unit length. Combining these statements with $dh = Tds + vdP$, the design-important quantity $\dot{S}'_{\text{gen}}$ becomes[3]

$$\dot{S}'_{\text{gen}} = \frac{q'\Delta T}{T^2(1+\Delta T/T)} + \frac{\dot{m}}{\rho T}\left(-\frac{dP}{dx}\right)$$

$$\cong \frac{q'\Delta T}{T^2} + \frac{\dot{m}}{\rho T}\left(-\frac{dP}{dx}\right) \geq 0 \tag{3}$$

The denominator of the first term on the right-hand side has been simplified by assuming that the local temperature difference ΔT is negligible compared with the local absolute temperature T.

The heat exchanger passage is a site for both flow with friction and heat transfer across a finite ΔT; this is why the $\dot{S}'_{\text{gen}}$ expression has two terms, each accounting for one irreversibility mechanism. We record this observation by rewriting Eq. (3) as

$$\dot{S}'_{\text{gen}} = \dot{S}'_{\text{gen},\Delta T} + \dot{S}'_{\text{gen},\Delta P} \tag{4}$$

In other words, the first term on the right-hand side of Eq. (3) represents the entropy generation contributed by heat transfer. The relative importance of the two irreversibility mechanisms is described by the *irreversibility distribution ratio* ϕ, which is

* Department of Mechanical Engineering and Materials Science, Duke University, Durham, North Carolina 27706, U.S.A.

Received 2 February 1987 and accepted for publication on 23 February 1987

† The principle of thermodynamically "isolating" the component being optimized is absolutely essential. Violations of this principle can lead to the type of "paradoxes" illustrated in the section "Heat Exchangers with Negligible Pressure Drop Irreversibility."

0142-727X/87/040258-19$03.00

Notation

a_1	Area constraint (Eq. 53)
A	Area, cross-sectional area, flow cross section
A_b	Gas-liquid bath contact area
A_g	Gas-atmosphere contact area
$A_{1,2}$	Areas of the two sides of the heat exchanger surface (Eq. 43)
b	Damping coefficient
B_0	Dimensionless group (Eq. 16)
c	Specific heat of solid or incompressible liquid
c_P	Specific heat at constant pressure, J/kg K
$\bar{c}_P$	Specific heat at constant pressure, J/kgmole K
C_D	Drag coefficient
C_i	Concentration, kgmole/m^3
C^*	Constant (Eq. 114)
D	Tube diameter, plate-to-plate spacing
D_h	Hydraulic diameter
D_i	Mass diffusivity
e_x	Specific flow exergy, J/kg
E_x	Flow exergy, J
$\dot{E}_x$	Flow exergy flowrate, W
f	Friction factor
F_D	Drag force
g	Dimensionless mass velocity (Eq. 51)
G	Mass velocity (Eq. 9)
h	Specific enthalpy, J/kg
$\bar{h}$	Heat transfer coefficient, W/m^2 K
$\mathbf{j}$	Mass flux vector, kgmole/m^{2}s
k	Thermal conductivity
k	Ratio of specific heats, c_P/c_v
K	Spring constant (Fig. 2)
K	Permeability of porous medium in the Darcy flow regime (Eq. 124)
L	Length
m	Mass
$\dot{m}$	Mass flowrate
$\dot{m}_r$	Mass flowrate during the exergy removal phase
M_p	Piston mass
N_k	Number of moles of species k
N_S	Entropy generation number
$N_{S,a}$	Augmentation entropy generation number
$N_{S,imbalance}$	Imbalance (remanent) entropy generation number
$N_{S,1}, N_{S,2}$	Entropy generation numbers of the two sides of the heat exchanger surface
Nu	Nusselt number
N_{tu}	Number of heat transfer units (Eq. 45)
p	Wetted perimeter, m (Eq. 11)
P	Pressure
P_i	Partial pressure of species i
P_0	Reference pressure
Pr	Prandtl number, ν/α
$\mathbf{q}$	Heat flux vector, W/m^2
q'	Heat transfer rate per unit length, W/m
q''	Heat flux, W/m^2
$\dot{Q}$	Heat transfer rate, W
$\dot{Q}_B$	Heat transfer rate from body to external flow
$\dot{Q}_0$	Heat transfer rate interaction with the ambient
r_{large}, r_{small}	Temperature ratios (Eq. 74)
R	Ideal gas constant, J/kg K
$\bar{R}$	Universal gas constant, J/kgmole K
Re	Reynolds number
s	Specific entropy, J/kg K
S	Entropy, J/K
$\dot{S}_{gen}$	Entropy generation rate, W/K
$\dot{S}'_{gen}$	Entropy generation rate per unit length, W/m K
s'''_{gen}	Volumetric entropy generation rate, W/m^3 K
$\bar{s}_i$	Partial molal entropy, J/k mole K
St	Stanton number
t	Time
t_c	Cooldown time
T	Temperature
T_B	Surface temperature of body in external flow
T_i	Initial temperature (Fig. 13)
T_L	Refrigerant (cold gas) temperature
T_0	Reference or ambient temperature
T_∞	Free stream temperature, gas supply temperature
u	Specific internal energy
U	Internal energy
U_∞	Free stream velocity
$\mathbf{v}$	Velocity vector
v_x, v_y	Velocity components
$\tilde{v}$	Parameter, m^3/kg (defined after Eq. 89)
v_1	Volume constraint (Eq. 58)
x, y, z	Cartesian coordinates
x	Quality
y	Dimensionless parameter (Eq. 109)
Z	Displacement
w'''	Volumetric rate of power dissipation, W/m^3
α	Thermal diffusivity
Δ	Difference
ε	Heat exchanger effectiveness (Eq. 78)
ε_R	Rational effectiveness (Eq. 94)
η_I	First-law efficiency (Eq. 103)
η_{II}	Second-law efficiency
$\eta_{W\text{-}S}$	Witte and Shamsundar's efficiency (Eq. 97)
θ	Dimensionless time (Eq. 106)
μ	Viscosity
μ_i	Chemical potential of species i
ν	Kinematic viscosity
ρ	Density
τ	Dimensionless temperature difference (Eqs. 48 and 106)
ϕ	Irreversibility distribution ratio (Eq. 5)
Φ	Viscous dissipation function (Eqs. 30 and 31)
ω	Capacity rate ratio, $(\dot{m}c_P)_1/(\dot{m}c_P)_2 > 1$
ω	$(K/M_p)^{1/2}$ (Fig. 2)

Subscripts

a	Augmented
b	Batch of liquid or solid storage material
B	Brayton-cycle power plant
C	Cooler, cold side
f	Saturated liquid, or final state
fg	Shorthand for $(\ )_g$-$(\ )_f$
g	Saturated vapor
H	Heater, hot side
i	Initial state, inner surface, species
in	Inlet
max	Maximum
min	Minimum
o	Outer surface
opt	Optimum
out	Outlet
pm	Fluid saturated porous medium
ΔP	Due to fluid flow ΔP
r	Removal phase of storage cycle
R	Regenerator
ΔT	Due to heat transfer ΔT
w	Wall
*	Dimensionless variables (Eq. 36)
0	Reference, ambient conditions

defined as

$$\phi = \frac{\text{fluid flow irreversibility}}{\text{heat transfer irreversibility}} \tag{5}$$

Equation (4) can then be rewritten as

$$\dot{S}'_{gen} = (1+\phi)\dot{S}'_{gen,\Delta T} \tag{6}$$

A remarkable feature of the $\dot{S}'_{gen}$ expression (Eq. 3), and of many like it for other simple devices, is that a proposed design change (for example, making the passage narrower) induces *changes of opposite signs* in the two terms of the expression. There exists then an *optimum tradeoff* between the two irreversibility contributions, an optimum design for which the overall measure of exergy destruction ($\dot{S}'_{gen}$) is minimum while the system continues to serve its specified function ($q', \dot{m}$).

The tradeoff between heat transfer and fluid flow irreversibilities becomes clearer if we convert Eq. (3) into the language of heat transfer engineering, in which the heat exchange passage is usually discussed. For this purpose, we recall the definitions of friction factor, Stanton number, mass velocity, Reynolds number, and hydraulic diameter

$$f = \frac{\rho D_h}{2G^2}\left(-\frac{dP}{dx}\right) \tag{7}$$

$$\mathrm{St} = \frac{q'/(p\Delta T)}{c_p G} \tag{8}$$

$$G = \frac{\dot{m}}{A} \tag{9}$$

$$\mathrm{Re} = \frac{GD_h}{\mu} \tag{10}$$

$$D_h = \frac{4A}{p} \tag{11}$$

where $q'/(p\Delta T)$ of Eq. (8) is the average heat transfer coefficient. The entropy generation rate formula (Eq. 3) becomes

$$\dot{S}'_{gen} = \frac{(q')^2 D_h}{4T^2 \dot{m} c_p \mathrm{St}} + \frac{2\dot{m}^3 f}{\rho^2 T D_h A^2} \tag{12}$$

Considering that both q' and $\dot{m}$ are fixed, we note that the thermodynamic design of the heat exchanger passage has two degrees of freedom, the wetted perimeter p and the cross-sectional area A, or any other pair of independent parameters, such as (Re, D_h) or (G, D_h).

The competition between heat transfer and fluid flow irreversibilities is hinted at by the positions occupied by St and f on the right-hand side of Eq. (12). The Reynolds and Colburn analogies regarding turbulent momentum and heat transfer teach us that St and f usually increase simultaneously,[4] as the designer seeks to improve the thermal contact between wall and fluid. Thus what is good for reducing the heat transfer irreversibility is bad for the fluid flow irreversibility, and vice versa.

The tradeoff between the two irreversibilities and the minimum value of the overall $\dot{S}'_{gen}$ can be illustrated by assuming a special case of passage geometry, namely, the straight tube with circular cross section. In this case, p and A are related through the pipe inner diameter D, the only degree of freedom left in the design process. Writing

$$D_h = D, \qquad A = \pi\frac{D^2}{4}, \quad \text{and} \quad p = \pi D \tag{13}$$

Eq. (12) becomes

$$\dot{S}'_{gen} = \frac{(q')^2}{\pi T^2 k \mathrm{Nu}} + \frac{32\dot{m}^3 f}{\pi^2 \rho^2 T D^5} \tag{14}$$

where $\mathrm{Re} = 4\dot{m}/(\pi\mu D)$, and $\mathrm{Nu} = \bar{h}D_h/k = \mathrm{St}\,\mathrm{Re}\,\mathrm{Pr}$. Invoking two reliable correlations for Nu and f in fully developed turbulent pipe flow, such as $\mathrm{Nu} = 0.023\,\mathrm{Re}^{0.8}\mathrm{Pr}^{0.4}$ and $f = 0.046\,\mathrm{Re}^{-0.2}$, and combining them with Eq. (14), yields an expression for $\dot{S}'_{gen}$ that depends only on Re. Solving $d\dot{S}'_{gen}/d(\mathrm{Re}) = 0$, we find the entropy generation rate is minimized when the Reynolds number (or pipe diameter) reaches the optimum value:[5]

$$\mathrm{Re}_{opt} = 2.023\,\mathrm{Pr}^{-0.071}\,B_0^{0.358} \tag{15}$$

This compact formula allows the designer to select the optimum tube size for minimum irreversibility. Parameter B_0 is fixed as soon as q', $\dot{m}$, and the working fluid are specified:

$$B_0 = \dot{m}q'\frac{\rho}{\mu^{5/2}(kT)^{1/2}} \tag{16}$$

The effect of Re on $\dot{S}'_{gen}$ can be expressed in relative terms as

$$\frac{\dot{S}'_{gen}}{\dot{S}'_{gen,min}} = 0.856\left(\frac{\mathrm{Re}}{\mathrm{Re}_{opt}}\right)^{-0.8} + 0.144\left(\frac{\mathrm{Re}}{\mathrm{Re}_{opt}}\right)^{4.8} \tag{17}$$

where $\dot{S}'_{gen,min} = \dot{S}'_{gen}(\mathrm{Re}_{opt})$.

Figure 1 shows that the entropy generation rate of the tube increases sharply on either side of the optimum. The irreversibility distribution ratio varies along the V-shaped curve, increasing in the direction of small D's (large Re's, because $\dot{m}$ = constant) in which the overall entropy generation rate is dominated by fluid friction effects. At the optimum, the irreversibility distribution ratio assumes the value $\phi_{opt} = 0.168$.

This most fundamental issue of thermodynamic irreversibility at the heat exchanger passage level was reconsidered by Kotas and Shakir.[6] They took into account the temperature dependence of transport properties and showed that the operating temperature of the heat exchanger passage has a profound effect on the thermodynamic optimum. For example, the optimum Reynolds number increases as the absolute temperature T decreases. The minimum irreversibility corresponding to this optimum design also increases as T decreases.

Heat transfer augmentation

Another example of the competition between different irreversibility mechanisms occurs in connection with the general problem of heat transfer augmentation, in which the main objective is to devise a technique that increases the wall–fluid heat transfer coefficient relative to the coefficient of the unaugmented (that is, untouched) surface. A parallel objective, however, is to register this improvement without causing a

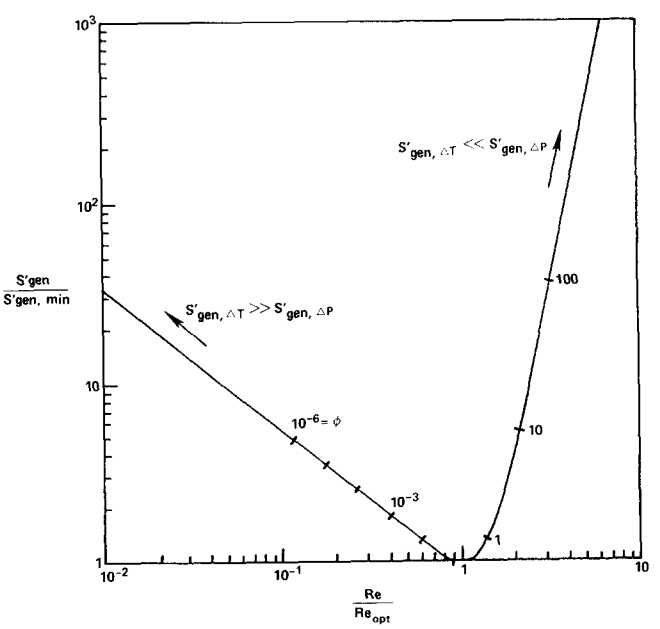

Figure 1 The relative entropy generation rate for forced convection heat transfer through a smooth tube

damaging increase in the pumping power demanded by the forced convection arrangement. These two objectives reveal the conflict that accompanies the application of any augmentation technique: A design modification that improves the thermal contact (for example, roughening the heat transfer surface) is likely to augment also the mechanical pumping power requirement.

The true effect of a proposed augmentation technique on thermodynamic performance may be evaluated by comparing the irreversibility of the heat exchange apparatus before and after the implementation of the augmentation technique.[7] Consider again the general heat exchanger passage referred to in Eqs. (1)–(3), and let $\dot{S}'_{\text{gen},0}$ represent the degree of irreversibility in the reference (unaugmented, untouched) passage. Writing $\dot{S}'_{\text{gen,a}}$ for the heat transfer-augmented version of the same device, we can evaluate the *augmentation entropy generation number* as

$$N_{S,\text{a}}=\frac{\dot{S}'_{\text{gen,a}}}{\dot{S}'_{\text{gen},0}} \tag{18}$$

Augmentation techniques whose $N_{S,\text{a}}$ values are less than 1 are thermodynamically advantageous.

If the function of the heat exchanger passage is fixed, that is, if $\dot{m}$ and q' are given, the augmentation entropy generation number can be put in the more explicit form

$$N_{S,\text{a}}=\frac{1}{1+\phi_0}N_{S,\Delta T}+\frac{\phi_0}{1+\phi_0}N_{S,\Delta P} \tag{19}$$

where ϕ_0 is the irreversibility distribution ratio of the reference design, and $N_{S,\Delta T}$ and $N_{S,\Delta P}$ represent the values of $N_{S,\text{a}}$ in the limits of pure heat transfer irreversibility and pure fluid flow irreversibility, respectively. It is not difficult to show that these limiting values are

$$N_{S,\Delta T}=\frac{\text{St}_0\,D_{\text{h,a}}}{\text{St}_\text{a}\,D_{\text{h},0}} \tag{20}$$

$$N_{S,\Delta P}=\frac{f_\text{a}D_{\text{h},0}A_0^2}{f_0D_{\text{h,a}}A_\text{a}^2} \tag{21}$$

The geometric parameters (A, D_h) before and after augmentation are linked through the $\dot{m}$=constant constraint, which reads

$$\text{Re}_\text{a}\frac{A_\text{a}}{D_{\text{h,a}}}=\text{Re}_0\frac{A_0}{D_{\text{h},0}} \tag{22}$$

Equations (19)–(22) show that $N_{S,\text{a}}$ is, in general, a function of both the heat transfer coefficient ratio ($\text{St}_\text{a}/\text{St}_0$) and the friction factor ratio (f_a/f_0). The relative importance of the friction factor ratio is dictated by the numerical value of ϕ_0: This value is known because the reference design is known. The $N_{S,\text{a}}$ calculation outlined above was used to evaluate several heat transfer augmentation techniques, ranging from surface roughening to the use of inserts that promote swirl flow.[7,8]

The impact of heat transfer augmentation on entropy generation was reconsidered more recently by Perez-Blanco.[9] In place of a passage of length dx, Perez-Blanco took as system a single-stream heat exchanger tube of finite length (L). For simplicity, he assumed the tube wall temperature is uniform and developed analytical means of calculating the overall entropy generation rate of the finite-size system in terms of potential design variables. Particularly interesting are the results showing the maximum friction factor range that can be tolerated during heat transfer enhancement to maintain an unchanged overall entropy generation rate.

External flow and heat transfer

The competition between flow and heat transfer irreversibilities rules also the thermodynamic design of external convection heat transfer arrangements, in which the flow engulfs the solid body (walls) it exchanges heat transfer with. The overall entropy generation rate associated with an external convection configuration is[10]

$$\dot{S}_\text{gen}=\frac{\dot{Q}_\text{B}(T_\text{B}-T_\infty)}{T_\infty T_\text{B}}+\frac{F_\text{D}U_\infty}{T_\infty} \tag{23}$$

where $\dot{Q}_\text{B}$, T_B, T_∞, F_D, and U_∞ are, respectively, the instantaneous heat transfer rate between the body and the fluid reservoir, the body surface temperature, the fluid reservoir temperature, the drag force, and the relative speed between body and reservoir.

This remarkably simple result proves again that inadequate thermal contact (the first term) and fluid friction (the second term) contribute hand in hand to degrading the thermodynamic performance of the external convection arrangement. One area in which Eq. (23) has found application is the problem of selecting the size and number (density) of fins for the design of extended surfaces. The thermodynamic optimization of fins and fin arrays of various geometries is described in Poulikakos.[10,11]

Convective heat transfer in general

What all the preceding examples have in common is a two-term expression for the entropy generation rate, or two distinct mechanisms of thermodynamic irreversibility: heat transfer and flow with friction. These two mechanisms are at work at any point in a convective field, as can be seen from the point-size control volume formulation of the mass conservation principle, the first law, and the second law:

$$\frac{\partial\rho}{\partial t}=-\rho\nabla\cdot\mathbf{v} \tag{24}$$

$$\rho\frac{\partial u}{\partial t}=-\nabla\cdot\mathbf{q}-P\nabla\cdot\mathbf{v}-w''' \tag{25}$$

$$s'''_\text{gen}=\rho\frac{\partial s}{\partial t}+\nabla\cdot\left(\frac{\mathbf{q}}{T}\right)\geqslant 0 \tag{26}$$

The vectors $\mathbf{v}$ and $\mathbf{q}$ represent the velocity and the heat flux at the point surrounded by the infinitesimally small control volume. Note also that w''' represents the work done by the system per unit time and per unit volume. Eliminating u and s between these laws and using the per-unit-time version of $du=Tds-Pdv$, namely,

$$\frac{\partial u}{\partial t}=T\frac{\partial s}{\partial t}+\frac{P}{\rho^2}\frac{\partial\rho}{\partial t} \tag{27}$$

yields the suspected two-term expression for the volumetric rate of entropy generation

$$s'''_\text{gen}=-\frac{1}{T^2}\mathbf{q}\cdot\nabla T-\frac{w'''}{T}\geqslant 0 \tag{28}$$

In the case of the incompressible flow of a viscous fluid, the place of $(-w''')$ in the first law (Eq. 25) is occupied by $\mu\Phi$, where Φ is the viscous dissipation function (ref. 4, p. 11). Further, the heat flux vector and the local temperature gradient are related through the Fourier law of thermal diffusion

$$\mathbf{q}=-k\nabla T \tag{29}$$

which means on the right-hand side of Eq. (28), both terms are positive:

$$s'''_\text{gen}=\frac{k}{T^2}(\nabla T)^2+\frac{\mu}{T}\Phi\geqslant 0 \tag{30}$$

This aspect becomes even more evident if we write the two-dimensional version of Eq. (30) for a flow field (x, y) in which the local velocity components are (v_x, v_y):

$$s'''_\text{gen}=\frac{k}{T^2}\left[\left(\frac{\partial T}{\partial x}\right)^2+\left(\frac{\partial T}{\partial y}\right)^2\right]+\frac{\mu}{T}\left\{2\left[\left(\frac{\partial v_x}{\partial x}\right)^2+\left(\frac{\partial v_y}{\partial y}\right)^2\right]+\left(\frac{\partial v_x}{\partial y}+\frac{\partial v_y}{\partial x}\right)^2\right\} \tag{31}$$

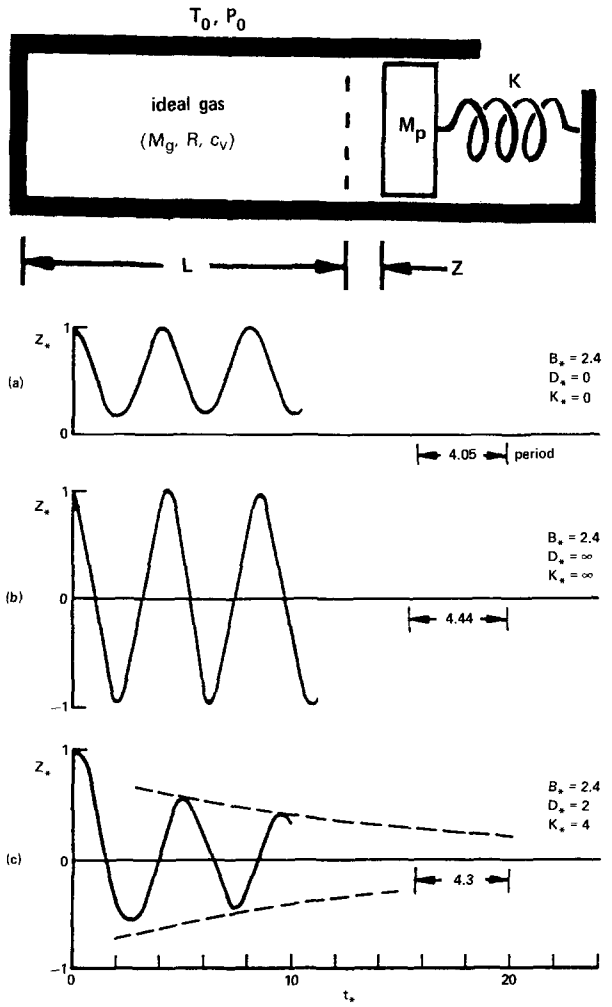

Figure 2 (a) and (b) Undamped oscillations of a spring-mass gas system. (c) Thermal damping as the fingerprint of entropy generation due to heat transfer

The first term on the right-hand side is clearly the contribution due to finite heat transfer down finite temperature gradients, and the second term represents the irreversibility due to frictional dissipation. This is why the finite control volume analyses highlighted in the preceding subsections led to similar two-term expressions for the entropy generation rate. The entropy generation rate of the finite-size control volume is the volume integral of the volumetric entropy generation rate s'''_{gen}. The manner in which a convective field generates entropy at every point in the flow can be illustrated by means of entropy generation profiles and maps.[1,2,12]

Thermal "damping"

On the pedagogical side of the challenge we face in engineering thermodynamics, one contribution of the irreversibility tradeoffs illustrated in this section is that they give physical meaning to relatively illusive concepts like the thermodynamic "loss" due to heat transfer across a finite ΔT. The two-term expressions seen above demonstrate that the heat transfer thermodynamic loss is directly comparable with a scaled version of the easier to grasp mechanical concept of frictional dissipation. The same lesson is taught by an ingenious exercise conceived by Moody[13] and summarized here in Figure 2.

Figure 2(a) shows a spring-mass system (K, M_p) whose mass can serve as a piston for compressing a batch of ideal gas (M_g, R, c_v). Disregarding the gas for a moment, we assume the piston slides in the cylindrical sleeve *with friction* in such a way that the friction force is proportional to the piston velocity. The motion of the piston is governed by the well-known equation

$$\frac{d^2Z}{dt^2}+b\frac{dZ}{dt}+\omega^2 Z=0 \tag{32}$$

where b is the damping coefficients and $\omega^2=K/M_p$. The motion is an undamped sinusoidal oscillation if $b=0$. In the general case $b>0$, the oscillation is damped, and the amplitude decreases exponentially in time:

$$Z=c_1\exp(-\tfrac{1}{2}bt)\sin\left\{\omega\left[1-\left(\frac{b}{2\omega}\right)^2\right]^{1/2}(t+c_2)\right\} \tag{33}$$

We shall see the same kind of damped oscillation is possible if $b=0$ and irreversibility is provided by a mechanism other than "sliding with friction." This time we assume that the leak-proof seal between the piston and cylinder is frictionless, and the ideal gas compresses and expands in response to the motion $Z(t)$. The entire apparatus is surrounded by the atmospheric temperature and pressure reservoir (T_0, P_0). Since the temperature of the ideal gas (T) is expected to vary, we model the instantaneous heat transfer rate between it and the atmosphere as

$$\dot{Q}_0=\bar{h}A_g(T-T_0) \tag{34}$$

Here A_g is the gas-atmosphere contact area, and $\bar{h}$ is the corresponding heat transfer coefficient. Using Moody's notation, the differential equation for the piston motion can be written as[13]

$$\frac{d^3Z_*}{dt_*^3}+D_*\frac{d^2Z_*}{dt_*^2}+B_*\frac{dZ_*}{dt_*}+K_*Z_*=0 \tag{35}$$

where the dimensionless variables are

$$t_*=t\left(\frac{AP_0}{M_pL}\right)^{1/2},\qquad B_*=k+\frac{KL}{AP_0},\qquad K_*=D_*\left(1+\frac{KL}{AP_0}\right)$$
$$D_*=(k-1)\frac{\bar{h}A_gT_0}{LAP_0}\left(\frac{M_pL}{AP_0}\right)^{1/2},\qquad Z_*=\frac{Z}{Z_0} \tag{36}$$

Other parameters used in this formulation are L (the rest length of the gas column), A (the cylinder cross-sectional area), and k (the ratio c_P/c_v of the gas, which should not be confused with the thermal conductivity). We focus next on three distinct regimes.

a. The reversible and adiabatic limit corresponds to $\bar{h}=0$, which means $D_*=K_*=0$, and Eq. (35) reduces to

$$\frac{d^2Z_*}{dt_*^2}+B_*Z_*=\text{constant} \tag{37}$$

In this case, the motion is a pure (undamped) sinusoid, as Figure 2(a) shows. The ideal gas expands and contracts reversibly and adiabatically, and the lack of irreversibility in the entire system is responsible for the absence of damping.

b. The reversible and isothermal limit is represented by $\bar{h}\to\infty$; hence, $(D_*, K_*)\to\infty$. In this limit, the equation of motion prescribes again an undamped oscillation:

$$\frac{d^2Z_*}{dt_*^2}+\left(1+\frac{KL}{AP_0}\right)Z_*=0 \tag{38}$$

One example of this motion is given in Figure 2(b). The oscillation is again undamped because of the lack of irreversibility in the system.

c. The general class of systems where $\bar{h}$ is finite can be called thermally damped because the oscillation has all the features revealed by the damped mechanical oscillator of Eq. (32). Figure 2(c) shows one numerical solution to the complete Eq. (35). The damping effect in this case is provided by exactly what was missing in the limits (**a**) and (**b**), namely, irreversibly or entropy generation. Since frictional effects have been ruled out, the only irreversibility mechanism present in regime (**c**) is the heat transfer $\dot{Q}_0$ across the finite temperature gap $(T-T_0)$.

The message of Moody's example is that from an overall system perspective, the effect of heat transfer irreversibility is qualitatively the same as that of friction-based irreversibility. In

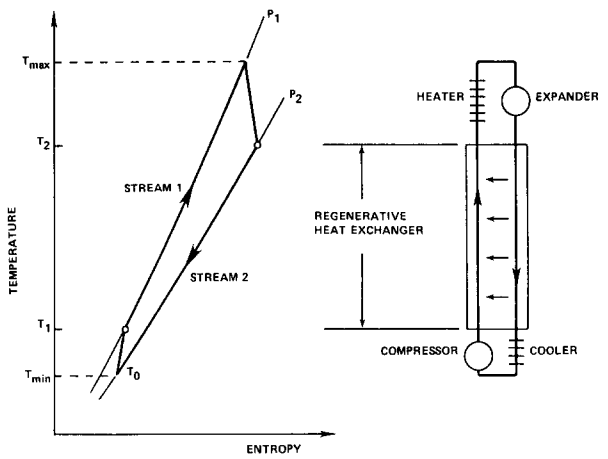

Figure 3 Brayton-cycle heat engine with regenerative (counter-flow) heat exchanger

Moody's example, that effect was damping. The message, however, is of general importance in thermodynamic design, and the effect of irreversibilities of all origins is always the same—lost exergy.

Balanced counterflow heat exchangers

In this section, we increase the degree of complexity of the system component and address the problem of irreversibility minimization in heat exchangers. The classical approach to heat exchanger design suffers from a traditional bias toward first-law analysis and against second-law consideration of any kind. The very name "heat exchanger" suggests that the function of the apparatus might be to transfer a certain amount of heat between two or more entities (streams most often) at different temperatures. This is not generally true. For example, in power and refrigeration cycles, the function of the heat exchanger equipment is to allow various components of the cycle to communicate with one another in the least irreversible way possible.

The ideal limit

The tradeoff between heat transfer and fluid flow irreversibilities becomes visible one more time if we consider the class of balanced counterflow heat exchangers in the ideal limit of small ΔP's and ΔT. "Balance" means the capacity flowrates are the same on the two sides of the heat transfer surface:

$$(\dot{m}c_P)_1=(\dot{m}c_P)_2=\dot{m}c_P \tag{39}$$

The two sides are indicated by the subscripts 1 and 2. With reference to the counterflow heat exchanger sketched in Figure 3, we write T_1 and T_2 for the fixed (given) inlet temperature of the two streams, and P_1 and P_2 for the respective inlet pressures. The entropy generation rate of the entire heat exchanger is

$$\dot{S}_{gen}=(\dot{m}c_P)_1\ln\frac{T_{1,out}}{T_1}+(\dot{m}c_P)_2\ln\frac{T_{2,out}}{T_2}-(\dot{m}R)_1\ln\frac{P_{1,out}}{P_1}-(\dot{m}R)_2\ln\frac{P_{2,out}}{P_2} \tag{40}$$

where the working fluid has been modeled as an ideal gas with constant specific heat. The outlet temperatures $T_{1,out}$ and $T_{2,out}$ can be eliminated by bringing in the concept of heat exchanger effectiveness.* If we also assume $(1-\varepsilon)\ll 1$, and that the pressure drops along each stream are sufficiently small relative to the absolute pressure levels, the entropy generation rate may be nondimensionalized as[2,14]

$$N_S=(1-\varepsilon)\frac{(T_2-T_1)^2}{T_1T_2}+\frac{R}{c_P}\left[\left(\frac{\Delta P}{P}\right)_1+\left(\frac{\Delta P}{P}\right)_2\right] \tag{41}$$

where N_S is the *entropy generation number*

$$N_S=\frac{1}{\dot{m}c_P}\dot{S}_{gen} \tag{42}$$

In this form, it is clear that the overall entropy generation rate (N_S) receives contributions from three sources of irreversibility, namely, the stream-to-stream heat transfer [regardless of the sign of (T_2-T_1)]; the pressure drop along the first stream, ΔP_1; and the pressure drop along the second stream, ΔP_2. The heat transfer irreversibility term can be split into two terms, each describing the contribution made by one side of the heat transfer surface. We are assuming that the stream-to-stream ΔT is due to the heat transfer across the two convective thermal resistances that sandwich the solid wall separating the two streams, and that the thermal resistance of the wall itself is negligible. That is, we write

$$\frac{1}{\bar{h}A_1}=\frac{1}{\bar{h}_1A_1}+\frac{1}{\bar{h}_2A_2} \tag{43}$$

where A_1 and A_2 are the heat transfer surface areas swept by each stream, and $\bar{h}_1$ and $\bar{h}_2$ the side-heat transfer coefficients based on these respective areas. The overall heat transfer coefficient $\bar{h}$ is based on A_1. The thermal resistance summation (Eq. 43) also means

$$\frac{1}{N_{tu}}=\frac{1}{N_{tu,1}}+\frac{1}{N_{tu,2}} \tag{44}$$

where

$$N_{tu}=\frac{\bar{h}A_1}{\dot{m}c_P},\qquad N_{tu,1}=\frac{\bar{h}_1A_1}{\dot{m}c_P},\qquad N_{tu,2}=\frac{\bar{h}_2A_2}{\dot{m}c_P} \tag{45}$$

In a balanced counterflow heat exchanger, the $\varepsilon(N_{tu})$ relationship is particularly simple[15]

$$\varepsilon=\frac{N_{tu}}{1+N_{tu}} \tag{46}$$

Combining Eqs. (41), (44), and (46), we find that in the "ideal" heat exchanger limit (small ΔT and ΔP's), the entropy generation number N_S splits into two groups of terms:

$$N_S=\underbrace{\frac{\tau^2}{N_{tu,1}}+\frac{R}{c_P}\left(\frac{\Delta P}{P}\right)_1}_{N_{S,1}}+\underbrace{\frac{\tau^2}{N_{tu,2}}+\frac{R}{c_P}\left(\frac{\Delta P}{P}\right)_2}_{N_{S,2}} \tag{47}$$

The contribution of the ideal-limit analysis is that it separates N_S into all the pieces that contribute to the irreversibility of the apparatus. The first pair of terms on the right-hand side of Eq. (47) represents the irreversibility contributed solely by side 1 of the heat transfer surface, $N_{S,1}$. The first term in this first pair is the entropy generation number due to heat transfer irreversibility on side 1, where τ^2 is shorthand for a parameter fixed by T_1 and T_2,

$$\tau^2=\frac{(T_2-T_1)^2}{T_1T_2} \tag{48}$$

The one-side entropy generation numbers $N_{S,1}$ and $N_{S,2}$ have the same analytical form; therefore, we can concentrate on the minimization of only one of them (say, $N_{S,1}$) and keep in mind that the minimization analysis can be repeated identically for $N_{S,2}$.

Despite the additive form of $N_{S,1}$ (Eq. 47), the heat transfer and fluid friction contributions to it are, in fact, coupled through the geometric parameters of the heat exchanger duct (passage) that resides on side 1 of the heat exchanger surface. This coupling is brought to light by rewriting $N_{S,1}$ in terms of the passage slenderness ratio $(4L/D_h)_1$:

$$N_{S,1}=\frac{\tau^2}{St_1}\left(\frac{D_h}{4L}\right)_1+\frac{R}{c_P}g_1^2f_1\left(\frac{4L}{D_h}\right)_1 \tag{49}$$

* The general effectiveness definition is listed in Eq (77)

where f_1 and St_1 are defined according to Eqs. (7) and (8). An important ingredient in the step from the $N_{S,1}$form (Eq. 47) to Eq. (49) is the relation between N_{tu} and St:

$$N_{tu,1}=\left(\frac{4L}{D_h}\right)_1 St_1 \tag{50}$$

which follows from the definitions (Eqs. 8, 11, and 45) in combination with $A_1=L_1p_1$, where p_1 is the wetted perimeter of passage 1. Finally, g_1 is a dimensionless mass velocity defined as

$$g_1=\frac{G_1}{(2\rho P_1)^{1/2}} \tag{51}$$

Area constraint

As summary to the ideal limit analyzed in the preceding section, we note the one-side irreversibility depends on two types of parameters:

$$\tau, \quad \frac{R}{c_P}, \quad Pr$$
$$\left(\frac{4L}{D_h}\right)_1, \quad Re_1, \quad g_1 \tag{52}$$

The first row contains the parameters fixed by the selection of working fluid and inlet conditions. The second row lists the three parameters that depend on the size and geometry of the heat exchanger passage. How many of these three parameters are true "degrees of freedom" depends on the number of design constraints.

One important constraint concerns the heat transfer area A_1. In dimensionless form, the constant-area condition may be expressed as[2]

$$a_1=\frac{A_1}{\dot m}(2\rho P_1)^{1/2}, \text{ constant} \tag{53}$$

where a_1 is the dimensionless area of side 1 of the surface. It is easy to show

$$a_1g_1=\left(\frac{4L}{D_h}\right)_1 \tag{54}$$

and only two degrees of freedom remain for the minimization of $N_{S,1}$:

$$N_{S,1}(g_1, Re_1)=\frac{\tau^2}{a_1g_1St_1}+\frac{R}{c_P}a_1f_1g_1^3 \tag{55}$$

Minimizing the entropy generation number subject to fixed (known) Reynolds number yields the optimum mass velocity

$$g_{1,opt}=\left[\frac{\tau^2}{(3R/c_P)a_1^2f_1\,St_1}\right]^{1/4} \tag{56}$$

$$N_{S,1,min}=\left[\frac{256\tau^6(Rc_P)f_1}{27a_1^2St_1^3}\right]^{1/4} \tag{57}$$

The minimum entropy generation number varies as $a_1^{-1/2}$; therefore, the thermodynamic goodness of the heat exchanger is enhanced by investing more area in the design of each side.

Volume constraint

The constant-volume constraint is important in the design of heat exchangers for applications where space is an expensive commodity (for example, power plants for naval and airborne applications). The dimensionless constant-volume constraint may be written as

$$v_1=V_1\frac{8P_1}{v\dot m}, \text{ constant} \tag{58}$$

where V_1 is the volume of the passage (duct) on side 1. Noting that V_1 equals L_1 times the cross-sectional flow area labeled A in Eqs. (9) and (11), we also have

$$v_1g_1^2=\left(\frac{4L}{D_h}\right)_1 Re_1 \tag{59}$$

This allows us to express $N_{S,1}$ in terms of only g_1 and Re_1 as degrees of freedom (Re_1 also governs the variation of St_1 and f_1):

$$N_{S,1}=\frac{\tau^2\,Re_1}{v_1g_1^2\,St_1}+\left(\frac{R}{c_P}\right)\frac{v_1f_1g_1^4}{Re_1} \tag{60}$$

Regarding Re_1 as given, the optimum mass flowrate and corresponding minimum irreversibility are[2]

$$g_{1,opt}=\left[\frac{\tau^2\,Re_1^2}{2(R/c_P)v_1^2f_1\,St_1}\right]^{1/6} \tag{61}$$

$$N_{S,1,min}=\left[\frac{27\tau^4(R/c_P)\,Re_1\,f_1}{4v_1\,St_1^2}\right]^{1/3} \tag{62}$$

The minimum irreversibility decreases as $v_1^{-1/3}$, that is, as the size of the flow passage increases and as the stream spends a longer time in residence in the passage.

Combined area and volume constraint

When the area (A_1) and the volume of the heat exchanger passage (V_1) are constrained simultaneously, only one degree of freedom is left for the thermodynamic optimization procedure (see the second row of Eq. (52)). This problem was formuated originally as an exercise.[16] Combining the area and volume constraints (Eq. 53 and 58) with the $N_{S,1}$ form collected from the right-hand side of Eq. (47), we obtain

$$N_{S,1}=\frac{\tau^2v_1}{a_1^2\,St_1\,Re_1}+\left(\frac{R}{c_P}\right)\frac{a_1^4f_1\,Re_1^3}{v_1^3} \tag{63}$$

Here the only variable is Re_1, which affects $N_{S,1}$ both directly and through St_1 and f_1. In some designs, St_1 and f_1 are relatively insensitive to changes in Re_1 (for example, in rough-wall pipes at sufficiently high Reynolds numbers). In these cases, the thermodynamic optimum corresponds to

$$Re_{1,opt}=\frac{v_1}{a_1^{3/2}}\left[\frac{\tau^2}{3(R/c_P)St_1f_1}\right]^{1/4} \tag{64}$$

It can be shown that the irreversibility distribution ratio ϕ at this optimum (that is, the second term of Eq. 63 divided by the first) is equal to 1/3.

N_{tu} constraint

Another way of exploiting the N_S-minimization idea was proposed recently by Sekulic and Herman.[17] What these authors consider fixed is the "operating point" in the heat transfer sense, that is, the overall number of heat transfer units (N_{tu}), the capacity flowrate ratio $[\omega=(\dot mc_P)_1/(\dot mc_P)_2]$, and the flow arrangement (counterflow, cross flow, and the like). Since, in general, the effectiveness is a function of N_{tu}, ω, and flow configuration, it means Sekulic and Herman's optimization is carried out also at constant ε.

In the case of a general two-stream heat exchanger (finite ΔT and ΔP's, unspecified flow arrangement), the entropy generation rate $\dot S_{gen}$ is given by Eq. (40), where the first two terms on the right-hand side account together for the heat transfer irreversibility, $\dot S_{gen,\Delta T}$. Writing

$$N_S=\frac{\dot S_{gen}}{(\dot mc_p)_2}, \qquad N_{S,\Delta T}=\frac{\dot S_{gen,\Delta T}}{(\dot mc_p)_2} \tag{65}$$

Table 1 The tradeoff between pressure drop irreversibilities in a heat exchanger with constnat overall N_{tu}

$\Delta\left(\frac{4L}{D_h}\right)_1$	→	$\Delta(N_{tu,1})$	→	$\Delta(N_{tu,2})$	→	$\Delta\left(\frac{4L}{D_h}\right)_2$	$\Delta(N_{S,\Delta P_1})$	→	$\Delta(N_{S,\Delta P_2})$
				Eq. (44), with N_{tu} = constant		Eq. (50) written for side 2			
		Eq. (50)						Conclusion	
(+)		(+)		(−)		(−)	(+)		(−)
(−)		(−)		(+)		(+)	(−)		(+)

Eq. (40) assumes the dimensionless form

$$N_S = N_{S,\Delta T} + \underbrace{\left[-\omega\left(\frac{R}{c_P}\right)_1 \ln\left(1-\frac{\Delta P_1}{P_1}\right)\right]}_{N_{S,\Delta P_1}} + \underbrace{\left[-\left(\frac{R}{c_P}\right)_2 \ln\left(1-\frac{\Delta P_2}{P_2}\right)\right]}_{N_{S,\Delta P_2}} \tag{66}$$

where $N_{S,\Delta P_1}$ and $N_{S,\Delta P_2}$ are clearly the pressure drop irreversibilities contributed by the two sides of the heat exchanger surface. The heat transfer entropy generation number $N_{S,\Delta T}$ is fixed in this case because it is, in general, a function of ε (or N_{tu}), ω, and flow arrangement. The special form taken by $N_{S,\Delta T}$ in the case of balanced counterflow heat exchangers in the ideal limit (small ΔT and ΔP's) is listed as the first term on the right-hand side of Eq. (41), or as the sum of the first and third terms in Eq. (47). The general $N_{S,\Delta T}$ expression for cross-flow heat exchangers is given by Sekulic and Herman.[17]

In conclusion, the overall irreversibility of the heat exchanger N_S varies on account of the two fluid flow irreversibilities, $N_{S,\Delta P_1}$ and $N_{S,\Delta P_2}$. These two flow terms are coupled through the constant-N_{tu} constraint (Eq. 44) so that there exists an optimum pair of flow-passage slenderness ratios for which N_S (or $N_{S,\Delta P_1}+N_{S,\Delta P_2}$) is minimum. The presence of this optimum is illustrated qualitatively in Table 1, where Δ represents the sign of the change in the indicated quantity.

Table 1 demonstrates that as the slenderness ratio of one passage increases, the slenderness of the companion passage decreases, and vice versa. The $N_{S,\Delta P}$-type terms of Eq. (66) increase monotonically with their respective $(4L/D_h)$ ratios, hence the conclusion constructed in the right of the table. The search for the thermodynamic optimum was carried out numerically for certain heat exchanger surfaces in cross flow:[17] A sample of this work is reproduced in Figure 4. The overall N_{tu} constraint is listed on each of the V-shaped curves. As N_{tu} increases, the optimum slenderness ratio of one side of the surface increases.

This optimization procedure of trading $N_{S,\Delta P_1}$ for $N_{S,\Delta P_2}$ makes sense as long as the overall N_S is dominated by pressure drop irreversibilities, that is, when $(N_{S,\Delta P_1}+N_{S,\Delta P_2}) \gg N_{S,\Delta T}$.

Heat exchangers with negligible pressure drop irreversibility

In this section, we take a closer look at the limit in which the $N_{S,\Delta P}$ terms are negligible in the general expression (Eq. 66)

$$N_S \cong N_{S,\Delta T} \tag{67}$$

Much of the attention being devoted to this limit in the literature is centered on the seemingly paradoxical conclusion that the irreversibility of these heat exchangers decreases both as $\varepsilon \to 1$ *and* as $\varepsilon \to 0$. I was the first to write about this paradox[5] in 1980 when I inked and published a pencil drawn example used by Professor Tribus in his Thermoeconomics class at M.I.T.[19] Back then I felt the origin of this paradox was clear and that the "entropy maximum" associated with it is of little practical consequence (see also ref. 1, pp. 28–29). In the meantime, this subject continued to draw attention in settings (configurations) considerably more general than the original balanced counterflow example. In fact, the essential idea of the existence of a maximum N_S versus ε was rediscovered independently on three other continents.[20–24]

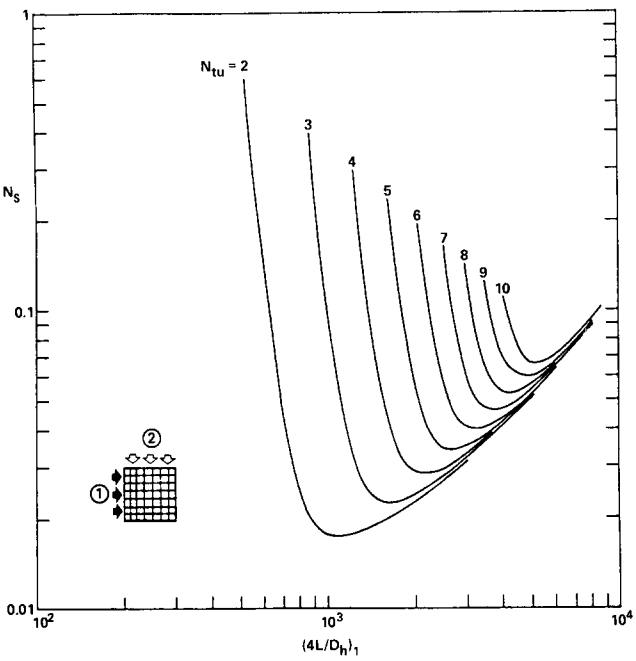

Figure 4 The minimization of entropy generation number subject to constant overall N_{tu} (results refer to a compact cross-flow heat exchanger with $\omega=0.5$; inlet temperature ratios $T_1/T_2=0.8$; and two surfaces,[18] namely, plate fin 11.1 and louvered fin 3/8–6.06)

Reconsidering the maximum entropy paradox[5] is useful because it constitutes an excellent illustration of the importance of the principle of thermodynamic "isolation" in the optimization of an engineering component. Consider again a balanced counterflow heat exchanger, for which in the limit of negligible pressure drop, the entropy generation rate (Eq. 40) reduces to a one-term entropy generation number:

$$N_S = \ln\left\{\left[1-\varepsilon\left(1-\frac{T_2}{T_1}\right)\right]\left[1+\varepsilon\left(\frac{T_1}{T_2}-1\right)\right]\right\} \tag{68}$$

Or using Eq. (46), N_S can be expressed as a function of the inlet temperature ratio and the overall N_{tu}:

$$N_S = \ln\frac{\left(1+\frac{T_1}{T_2}N_{tu}\right)\left(1+\frac{T_2}{T_1}N_{tu}\right)}{(1+N_{tu})^2} \tag{69}$$

Figure 5 illustrates the behavior of N_S at constant T_1/T_2. The entropy generation number is 0 at both $\varepsilon=0$ and $\varepsilon=1$, and its maximum is situated exactly at $\varepsilon=1/2$ (or at $N_{tu}=1$). The maximum entropy generation number increases as soon as T_1/T_2 goes above or below 1:

$$N_{S,max} = \ln\left[\frac{1}{2}+\frac{1}{4}\left(\frac{T_1}{T_2}+\frac{T_2}{T_1}\right)\right] \tag{70}$$

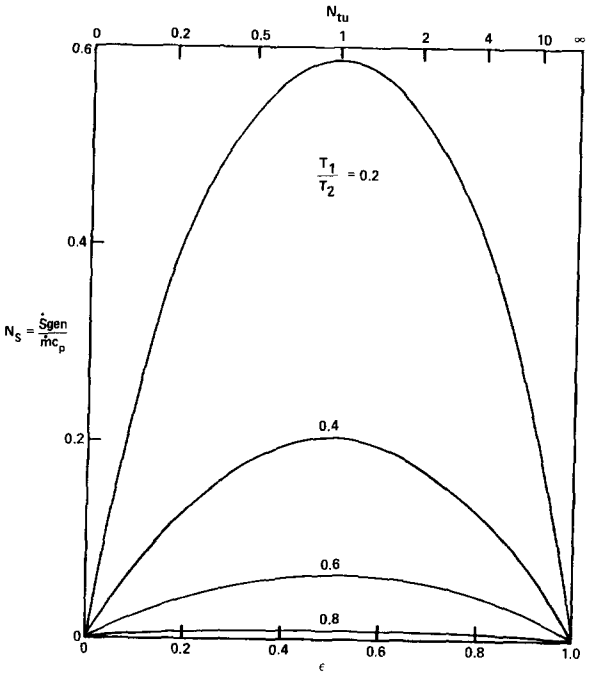

Figure 5 Entropy generation rate in a balanced counterflow heat exchanger with zero pressure-drop irreversibility

The behavior of N_S in the "good" heat exchanger limit ($\varepsilon \to 1$) is well understood and is expected. The behavior in the $\varepsilon \to 0$ extreme, however, is neither expected nor intuitively obvious because we expect any heat transfer irreversibility to increase monotonically as the heat exchanger area (or N_{tu}) decreases. One physical explanation for the anomalous behavior exhibited in Figure 5 is that in the $\varepsilon \to 0$ limit, the stream-to-stream temperature difference ΔT is practically constant and equal to $|T_1 - T_2|$. That is, ΔT is insensitive to the vanishing N_{tu}. Thus as N_{tu} and the heat exchanger area approach zero, the total heat transfer rate between the two streams decreases, as does the heat transfer irreversibility. The vanishing N_S seen in the limit $\varepsilon \to 0$ is first and foremost a sign that the heat exchanger *disappears* as an engineering component. So if $\varepsilon \to 1$ is the good heat exchanger limit, we can view $\varepsilon \to 0$ as the "absent heat exchanger limit."

Heat exchangers, in general, contribute to the overall irreversibility of the installations that incorporate them. The lower left-hand corner of Figure 5 is technically correct because an absent heat exchanger ($\varepsilon = 0$) can contribute only zero irreversibility as a heat exchanger ($N_S = 0$). However, if we think of the power and refrigeration applications that over the past two hundred years defined the need for inventing heat exchangers, we begin to appreciate the error in associating goodness with the declining-N_S trend observed toward $\varepsilon = 0$. Zero irreversibility is certainly good if the heat exchanger exists and does its job; however, a vanishing heat exchanger will definitely have a negative effect on the overall irreversibility of the mother system.

The absent heat exchanger limit ($\varepsilon \to 0$) is a territory in which the design changes experienced by the vanishing heat exchanger have a profound effect on the irreversibility of the system components the heat exchanger is in direct communication with. To see how the analysis of the entropy maximum violates the principle of system isolation, consider the greater problem of minimizing the irreversibility of the Brayton-cycle power plant seen already in Figure 3. The power plant has five components: the heater (H), expander, regenerator (R), cooler (C), and compressor. The regenerator (R) is the balanced counterflow heat exchanger Figure 5 was drawn for. For simplicity, we assume the expander and compressor function reversibly and adiabatically so that the entropy generation of the entire Brayton-cycle power plant (B) has only three components:

$$\dot{S}_{gen,B} = \dot{S}_{gen,H} + \dot{S}_{gen,R} + \dot{S}_{gen,C} \tag{71}$$

Dividing by the capacity flowrate $\dot{m}c_P$ (constant), we also have

$$N_{S,B} = N_{S,H} + N_{S,R} + N_{S,C} \tag{72}$$

The $N_{S,R}$ contribution was labeled N_S in Eqs. (68) and (69). Moreover, since the expander and compressor function isentropically, the traces left by them on the TS diagram of Figure 3 would be represented by vertical segments in the Brayton cycle.

Modeling the working fluid as an ideal gas with constant specific heat, it is a simple matter to show that the heat engine (first-law) efficiency of the power plant (η) depends on three dimensionless parameters: the regenerator effectiveness, ε; the overall temperature ratio T_{max}/T_{min}; and the absolute temperature ratio across the expander or compressor. The last is fixed by the pressure ratio, which is assumed given:

$$\frac{T_{max}}{T_2} = \frac{T_1}{T_{min}} = \left(\frac{P_1}{P_2}\right)^{R/c_P} \tag{73}$$

The first-law efficiency formula turns out to be

$$\eta = \frac{r_{large}(1 - r_{small}^{-1}) - r_{small} + 1}{r_{large}(1 - \varepsilon r_{small}^{-1}) - (1 - \varepsilon) r_{small}} \tag{74}$$

where $r_{large} = T_{max}/T_{min}$, and $r_{small} = T_{max}/T_2$.

Figure 6(a) proves what we expected from the beginning: "More" regenerator (larger ε) is always better from the viewpoint of upgrading the efficiency of the entire power system. Figure 6(b) shows, first, that the irreversibility of the entire system ($N_{S,B}$) decreases monotonically as ε increases (this agrees with Figure 6(a) and the Guoy-Stodola theorem[2]). Figure 6(b) also

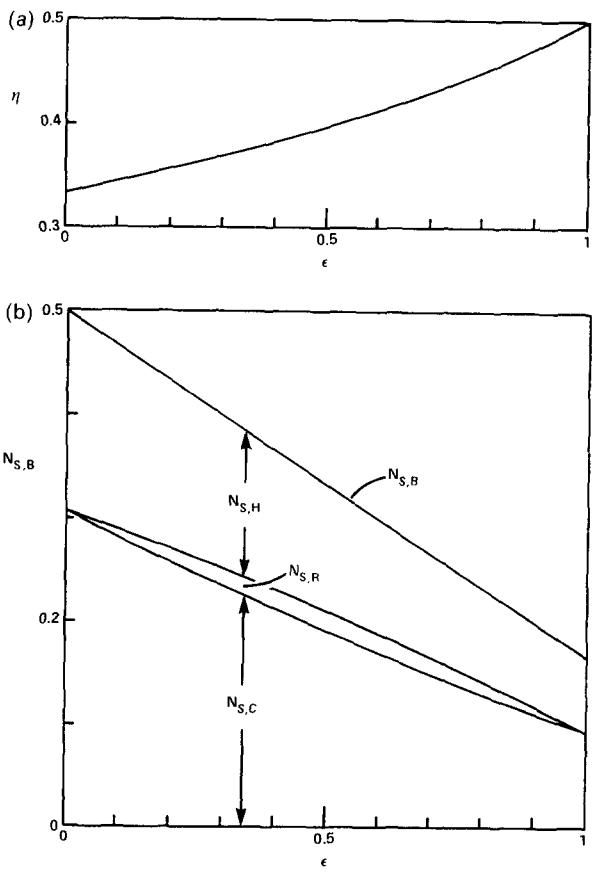

Figure 6 (a) The monotonic dependence between Brayton-cycle power plant efficiency and the size of the regenerative counterflow heat exchanger (drawn for $r_{large} = 3$ and $r_{small} = 3/2$; hence, $T_1/T_2 = 0.75$). (b) The distribution of power plant irreversibility among the three heat exchangers (H), (R), and (C).

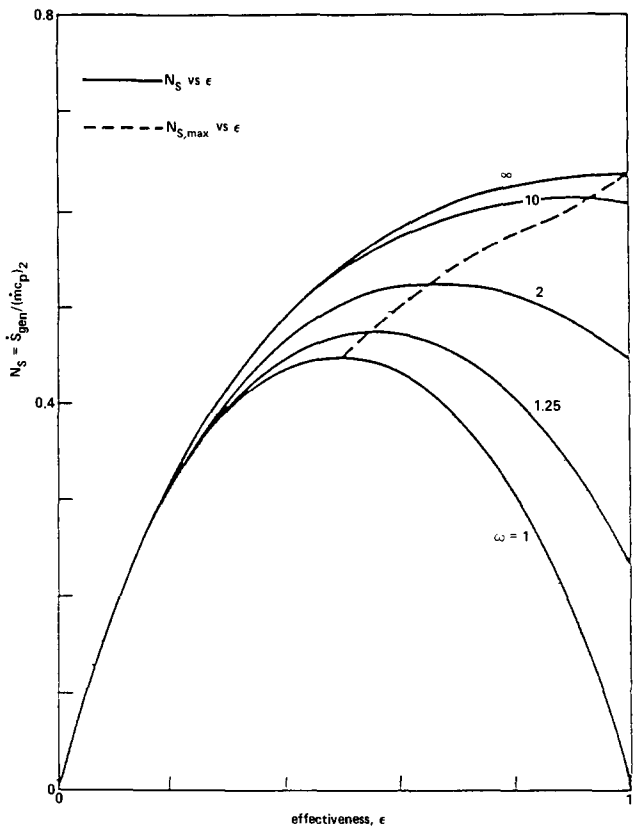

Figure 7 The irreversibility of imbalanced counterflow heat exchangers with negligible pressure drop irreversibility and $T_1/T_2=0.25$

shows the manner in which $N_{S,B}$ is distributed among the three heat exchangers (H), (R), and (C). The heater entropy generation rate was calculated assuming the heat input originates from T_{max} and the outlet temperature of the heated stream (that is, the inlet to the expander) equals T_{max}. That is, the heater is assumed to have an infinite number of heat transfer units. An identical model was used for the cooler, where the outlet temperature of the cooled stream equals the temperature of the cold side of the cooler, T_{min}.

Sandwiched between $N_{S,H}$ and $N_{S,C}$ is the irreversibility contribution made by the regenerator: This slice has exactly the same features as the $T_1/T_2=0.75$ curve that could be drawn near the base of Figure 5, namely, zero height at $\varepsilon=0$ and $\varepsilon=1$, and a maximum at $\varepsilon=1/2$. It is now clear that as ε decreases below 1/2, the vanishing of the regenerator has the effect of *augmenting* the heat transfer irreversibilities contributed by the surviving heat exhangers so that, overall, the irreversibility of the power plant increases monotonically. The only practical significance I can attach to the maximum thickness exhibited by the $N_{S,R}$ slice is that it marks the order of magnitude of ε (or N_{tu}) below which the analysis of the regenerator alone is a clear violation* of the principle of thermodynamic isolation.

The heat transfer irreversibility maximum illustrated here for balanced counterflow heat exchangers reappears in the analysis of other heat exchanger configurations. For example, Sarangi and Chowdhury[20] found it in imbalanced counterflow heat exchangers, that is, when $(\dot{m}c_P)_1 \neq (\dot{m}c_P)_2$. Their results are illustrated in Figure 7, where N_S is based on the smaller of the two capacity rates, $(\dot{m}c_P)_2$. Sekulic and Baclic[21] plotted it for counterflow and cross-flow heat exchangers, showing also that the maximum occurs at $\varepsilon=1$ in parallel flow heat exchangers. This last conclusion was drawn also by da Costa and Saboya[22] in a comparative study of $N_{S,\Delta T}$ for imbalanced counterflow and parallel flow heat exchangers. The presence of the entropy-maximum feature in the irreversibility of cross-flow heat exchangers with negligible pressure drop irreversibility is illustrated in Figure 8, where the N_S value of each configuration has been divided by the respective maximum N_S.

Remanent (flow imbalance) irreversibilities

The study of balanced counterflow heat exchangers led to the conclusion that the overall irreversibility of the device decreases to zero as the design approaches the ideal limit of infinite overall N_{tu} and zero ΔP on both sides of the surface. In this section, we focus strictly on the "perfect" design

$$N_{tu}=\infty, \qquad \Delta P_1=\Delta P_2=0 \tag{75}$$

and our objective is to show that in this limit the heat exchanger configurations that are not "balanced counterflow" are characterized by an unavoidable irreversibility solely due to the flow arrangement. For historical reasons,[14] and for lack of a better name, we refer to this remanent irreversibility as the *irreversibility due to flow imbalance* or *remanent irreversibility*.

Consider first an *imbalanced counterflow heat exchanger*, where

$$\omega=\frac{(\dot{m}c_P)_1}{(\dot{m}c_P)_2}>1 \tag{76}$$

and where the perfect design (Eq. 75) means $P_{1,out}=P_1$, $P_{2,out}=P_2$, and $\varepsilon=1$. The effectiveness-N_{tu} relations for imbalanced counterflow heat exchangers are

$$N_{tu}=\frac{\bar{h}A_1}{(\dot{m}c_P)_2}, \qquad \varepsilon=\omega\frac{T_1-T_{1,out}}{T_1-T_2}=\frac{T_{2,out}-T_2}{T_1-T_2} \tag{77}$$

$$\varepsilon=\frac{1-\exp[-N_{tu}(1-\omega^{-1})]}{1-\omega^{-1}\exp[-N_{tu}(1-\omega^{-1})]} \tag{78}$$

where $(\dot{m}c_P)_2$ is the smaller of the two capacity flowrates. In this

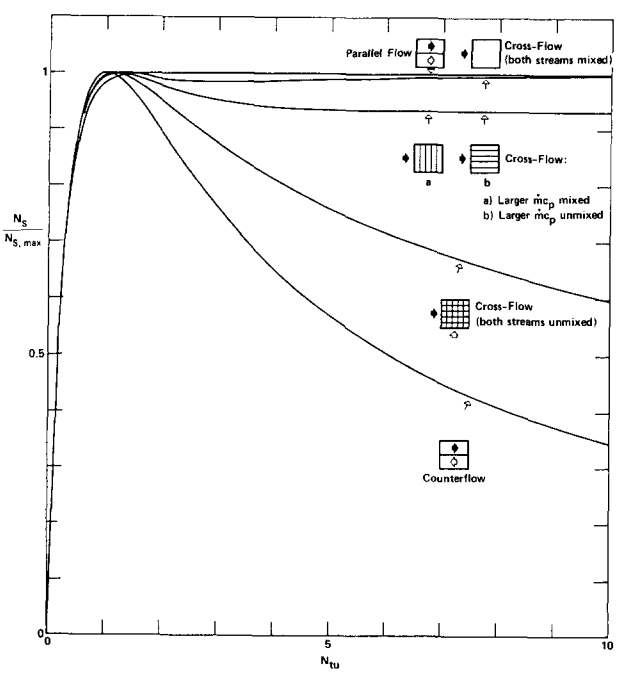

Figure 8 The occurrence of a maximum in the irreversibility of various heat exchanger configurations in which the pressure drop irreversibility is negligible ($T_1/T_2=0.5$, $\omega=1$)

* Indeed, the reason the ideal-limit optimization rules of the preceding section enjoy general validity is that the assumption of vanishingly small ΔT and ΔP's makes the outlet conditions of the two streams practically insensitive to the optimization work performed inside the heat exchanger, that is, insensitive to the changes in the already small ΔT and ΔP's. This decision effectively isolates the counterflow heat exchanger from the rest of the power or refrigeration installation it may belong to.

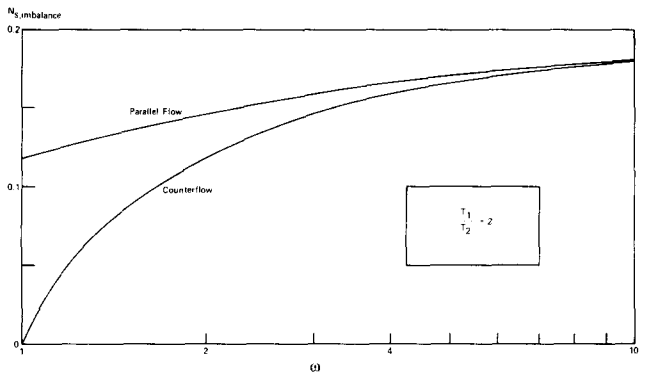

Figure 9 The remanent (flow imbalance) irreversibility in parallel flow is consistently greater than in counterflow; $\omega = (\dot{m}c_p)_1/(\dot{m}c_p)_2 > 1$

case, the overall entropy generation rate (Eq. 40) has a finite value

$$N_{S,\text{imbalance}} = \frac{\dot{S}_{\text{gen}}}{(\dot{m}c_P)_2} = \ln\left\{\left[1 - \frac{1}{\omega}\left(1 - \frac{T_2}{T_1}\right)\right]^{\omega}\frac{T_1}{T_2}\right\} \tag{79}$$

The imbalance irreversibility of a two-stream *heat exchanger with phase-change on one side* is a special case of Eq. (79), namely, the limit $\omega \to \infty$, where the stream that bathes side 1 does not experience a temperature variation from inlet to outlet, $T_{1,\text{out}} = T_1$. For this class of heat exchangers, Eq. (79) reduces to

$$N_{S,\text{imbalance}} = \frac{T_2}{T_1} - 1 - \ln\frac{T_2}{T_1}, \qquad (\omega = \infty) \tag{80}$$

The imbalance irreversibility of two-stream *parallel flow heat exchangers* is obtained similarly, by combining Eq. (40) with the perfect-design conditions (Eq. 75) and the $\varepsilon(\omega, N_{\text{tu}})$ relation for parallel flow:[15]

$$\varepsilon = \frac{1 - \exp[-N_{\text{tu}}(1 + \omega^{-1})]}{1 + \omega^{-1}} \tag{81}$$

The resulting expression is

$$N_{S,\text{imbalance}} = \frac{\dot{S}_{\text{gen}}}{(\dot{m}c_p)_2} = \ln\left\{\left(\frac{T_2}{T_1}\right)^{\omega}\left[1 + \left(\frac{T_1}{T_2} - 1\right)\frac{\omega}{1+\omega}\right]^{1+\omega}\right\} \tag{82}$$

A first observation is that in the limit of extreme imbalance ($\omega \to \infty$), this expression becomes the same as Eq. (80). In this limit, of course, the side 1 stream is so large that its temperature remains equal to T_1 from inlet to outlet; seen from the outside, it behaves like a stream that condenses or evaporates isobarically.

A second worthwhile observation is that when the two streams and their inlet conditions are given, the imbalance irreversibility of the parallel flow arrangement is consistently greater than the imbalance irreversibility of the counterflow scheme (Eq. 79). Figure 9 shows the behavior of the respective entropy generation numbers and how they both approach the value indicated by Eq. (80) as the flow imbalance ratio ω increases. Taking the $\omega = 1$ limit of Eq. (82), it is easy to see that the remanent irreversibility of the parallel flow arrangement is finite even in the balanced flow case (see also $\omega = 1$ in Figure 9).

Overview: the structure of heat exchanger irreversibility

An important structure should be recognized in the heat exchanger irreversibility treatment reviewed in the preceding three sections. First, there is the competition between heat transfer and fluid flow (pressure drop) irreversibilities, whose various tradeoffs were illustrated by considering the analytically simple limit of nearly ideal balanced counterflow heat exchangers. Second, it is essential to keep track of whether the

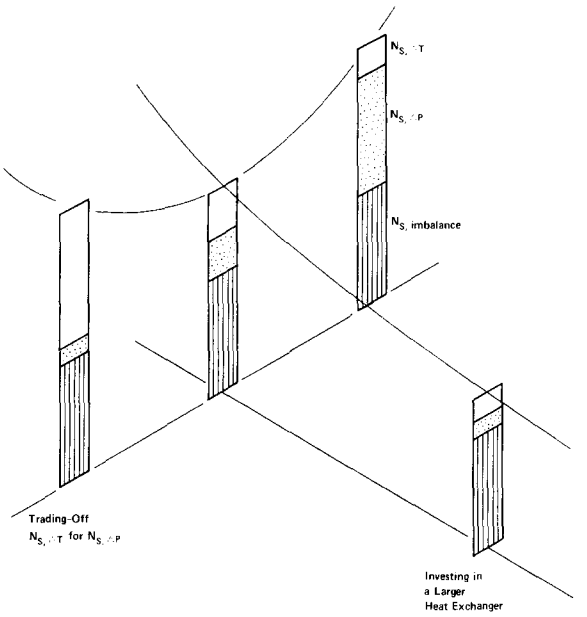

Figure 10 The structure of the total entropy generation rate of a heat exchanger

optimization of one heat exchanger causes the thermodynamic degradation of other components it might be hooked up to in the greater engineering system. We saw the violation of the principle of proper isolation by reexamining the maximum-entropy paradox of heat exchangers with zero pressure drop irreversibility. Finally, there is the recognition of remanent or flow imbalance irreversibilities, that is, irreversibilities that persist even in the limit of perfect heat exchangers (Eq. 75).

Figure 10 summarizes this structure. The remanent irreversibility deserves to be calculated first in the thermodynamic optimization of any heat exchanger because it establishes the level (order of magnitude) below which the joint minimization of heat transfer (finite ΔT, or N_{tu}) and fluid flow (finite ΔP) irreversibilities falls in the realm of diminishing returns. That is, it would no longer make sense to invest heat exchanger area and "engineering" into minimizing the sum $(N_{S,\Delta T} + N_{S,\Delta P})$ when this sum* is already negligible compared with the remanent irreversibility $N_{S,\text{imbalance}}$.

Only in very special cases does the entropy generation rate of a heat exchanger break up explicitly into a sum of three terms so that each term accounts for one of the irreversibilities reviewed above:

$$N_S = N_{S,\text{imbalance}} + N_{S,\Delta T} + N_{S,\Delta P} \tag{83}$$

One such case is the balanced counterflow heat exchanger in the nearly balanced and nearly ideal limit ($\omega \to 1, \Delta T \to 0, \Delta P\text{'s} \to 0$). In general, these three irreversibilities contribute in a more complicated way to the eventual size of the overall N_S. Deep down, however, the behavior of the three is the same as that of the simple limits singled out for discussion. Figure 10 illustrates this behavior qualitatively.

Two-phase flow heat exchangers

The analysis of other classes of heat exchangers reveals the basic structure outlined in Figure 10. One important class is the heat exchangers in which at least one of the streams is a two-phase mixture. (The irreversibility characteristics of this class were discussed first by Bejan[25] and, independently, by London and Shah.[26] Detailed sizing rules for thermodynamic and

* In this summary, $N_{S,\Delta P}$ is shorthand notation for the combined effect of pressure drop irreversibilities (for example, the sum in the square brackets of Eq. 41).

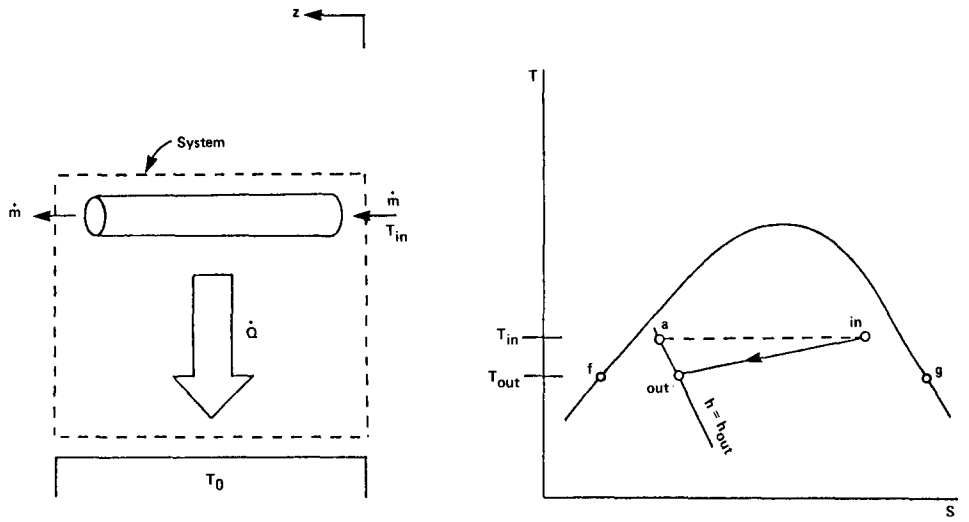

Figure 11 Entropy generation analysis of two-phase flow through a heat exchanger duct

thermoeconomic optimization were developed by Zubair *et al.*[27])

Consider Figure 11, which shows the steady flow of a two-phase mixture through a duct in thermal contact with a heat reservoir of temperature T_0. To understand the functioning of this heat exchanger, think of the condenser in a Rankine-cycle power plant, where T_0 is the absolute temperature of the atmosphere. The result of the following analysis, however, is quite general. Invoking the first law and the second law for the dashed-line control volume shown in Figure 11(a), we find the total entropy generation rate is

$$\dot{S}_{gen} = \dot{m}(s_{out} - s_{in}) + \frac{\dot{m}(h_{in} - h_{out})}{T_0} \geq 0 \tag{84}$$

where $\dot{m}(h_{in} - h_{out})$ is heat rejection rate to the ambient, $\dot{Q}$. From a design standpoint, we are interested in how the pressure drop ($\Delta P = P_{in} - P_{out}$) and the fluid-ambient temperature difference ($\Delta T = T_{in} - T_0$) affect the overall irreversibility level, $\dot{S}_{gen}$. Assuming the inlet and outlet states are both in the two-phase domain (Figure 11), we write

$$s_{out} - s_{in} = (s_a - s_{in}) + (s_{out} - s_a) \tag{85}$$

where the auxiliary state (a) is defined by the two properties

$$T_a = T_{in} \quad \text{and} \quad h_a = h_{out} \tag{86}$$

That is, the auxiliary state (a) represents the outlet state (out) in the theoretical limit of zero pressure drop. We note further

$$\begin{aligned} T_{in}(s_a - s_{in}) &= h_a - h_{in} \\ &= h_{out} - h_{in} \end{aligned} \tag{87}$$

Combining Eqs. (84)–(87), we find that the entropy generation rate separates into two terms:

$$\dot{S}_{gen} = \dot{Q}\left(\frac{1}{T_0} - \frac{1}{T_{in}}\right) + \dot{m}(s_{out} - s_a) \tag{88}$$

where, quite visibly, the first term represents the contribution due to imperfect stream-ambient thermal contact, whereas the second term accounts for the pressure drop irreversibility. In the limit of sufficiently small ΔP, the relationship between $(s_{out} - s_a)$ and ΔP can be expressed analytically as

$$s_{out} - s_a = [h_f' - T_{in}s_f' + x_{out}(h_{fg}' - T_{in}s_{fg}')]\frac{\Delta P}{T_{in}} \tag{89}$$

where the prime means $d(\ )/dP$, and x_{out} is the quality of the outflowing mixture. Properties at saturation such as h_f, s_f, h_{fg}, and s_{fg}, are known functions of pressure (or temperature). Therefore, the quantity in the square brackets in Eq. (89) can be calculated once the absolute pressure and the outlet quality are known. The quantity calculated in this manner has the units of specific volume; for it, we therefore may substitute the shorthand notation $\tilde{v}(P_{in}, x_{out})$. Using this new notation, the entropy generation rate assumes now a more familiar form:

$$\dot{S}_{gen} = \underbrace{\dot{Q}\frac{\Delta T}{T_{in}T_0}}_{\text{heat transfer irreversibility}} + \underbrace{\frac{\dot{m}\tilde{v}}{T_{in}}\Delta P}_{\text{fluid flow irreversibility}} \tag{90}$$

Repeating the analysis for a duct of length dz, where the longitudinal coordinate z is measured in the direction of the flowrate $\dot{m}$, we obtain the per-unit-length result

$$\frac{d\dot{S}_{gen}}{dz} = \frac{\Delta T}{T_{in}^2}\frac{d\dot{Q}}{dz} + \frac{\dot{m}\tilde{v}}{T_{in}}\left(-\frac{dP}{dz}\right) \tag{91}$$

This result contains the additional assumption that $(T_{in} - T_0) \ll T_{in}$. The structure of Eq. (91) is the same as that of entropy generation formulas encountered earlier. Therefore, by combining Eq. (91) with appropriate correlations for heat transfer coefficient and pressure drop in two-phase flow, it is possible to select a design (for example, duct inner diameter) so that $d\dot{S}_{gen}/dz$ is minimum.

If the duct of Figure 11 is surrounded by still air, and if T_w is the wall temperature, the local rate of entropy generation becomes[25]

$$\frac{d\dot{S}_{gen}}{dz} = \left(\frac{d\dot{Q}/dz}{T_{in}}\right)^2\left[\frac{1}{(p\bar{h})_i} + \frac{1}{(p\bar{h})_o}\right] + \frac{\dot{m}\tilde{v}}{T_{in}}\left(-\frac{dP}{dz}\right) \tag{92}$$

In this expression, p and $\bar{h}$ denote the wetted perimeter of the duct cross section and the heat transfer coefficient, and subscripts i and o stand, respectively, for the inner side and outer side of the duct wall. In writing only one pressure drop term in Eq. (92), we are assuming the flow outside the duct is driven by buoyancy effects. The entropy generation rate is due to only three contributors: the imperfect thermal contact between two-phase mixture and wall, the imperfect thermal contact between wall and ambient, and finally, the flow with friction through the duct.

If the tube of Figure 11 is surrounded not by a stagnant fluid reservoir but by an evaporating stream at a lower temperature, the entropy generation rate for this two-stream heat exchanger is[25]

$$\begin{aligned} \frac{d\dot{S}_{gen}}{dz} = &\left[\frac{1}{T^2p\bar{h}}\left(\frac{d\dot{Q}}{dz}\right)^2 + \frac{\dot{m}\tilde{v}}{T}\left(-\frac{dP}{dz}\right)\right]_H \\ &+ \left[\frac{1}{T^2p\bar{h}}\left(\frac{d\dot{Q}}{dz}\right)^2 + \frac{\dot{m}\tilde{v}}{T}\left(-\frac{dP}{dz}\right)\right]_C \end{aligned} \tag{93}$$

where subscripts H and C represent, respectively, the

condensing (hot) and evaporating (cold) sides of the heat exchanger surface. Note further the first law of thermodynamics requires $(d\dot{Q}/dz)_H = (d\dot{Q}/dz)_C$. The competition between heat transfer and fluid flow irreversibilities, or the opportunity for reaching a thermodynamic optimum based on the proper selection of duct geometry, is evident in both groups of terms on the right-hand side of Eq. (93).

Finally, regarding the shorthand notation $\tilde{v}$ for the quantity in the square brackets in Eq. (89), it is important to keep in mind the geometrical layout of the Ts diagram of Figure 11, on which the $\tilde{v}$ expression is based. Regardless of whether the process (in)→(out) represents condensation or evaporation, it was assumed that the fictitious isenthalpic process (a)→(out) is situated fully inside the two-phase dome. If the tube of Figure 11 works as a *condenser*, the outlet state will be situated on the left-hand frontier of the dome; that is, (out) ≡ ((f). In this case, the role of (a) will be played by a slightly subcooled (compressed) liquid state, and the process (a)→(out) will be executed by a single-phase stream. Invoking $dh = Tds + vdP$ and the constancy of enthalpy from (a) to (out), it is easy to prove that when (out) means saturated liquid, $\tilde{v}$ must be replaced by v_f.

Similarly, if the stream boils so that the outlet state is a single-phase saturated vapor state, (out) is replaced by a state (g) situated on the right-hand side of the two-phase dome. If the orientation of the constant-enthalpy line that passes through (g) is such that (a) would be situated outside the dome (to the right), then, based on the argument of the preceding paragraph, $\tilde{v}$ is replaced by v_g. Conversely, if the orientation of the constant-enthalpy line would make (a) fall inside the dome, the correct $\tilde{v}$ expression is the one listed in square brackets in Eq. (89). In this last case, $x_{out} = 1$.

Other heat exchanger configurations and ways of measuring irreversibility

In the years since the pioneering papers of the 1970s, the calculation and minimization of irreversibility in heat exchanger design has become a self-standing topic that continues to gather momentum. For example, this topic recently attracted Professor London,[28] a creative, influential figure whose long Stanford career had a lot to do with the streamlining and popularization of *first-law* analysis in heat exchanger design. Through him, the language of second-law analysis was spoken also in the prestigious Max Jakob Award acceptance lecture (Denver, 1985). In this section, we review several additional advances in heat exchanger second-law analysis, placing special emphasis on alternative approaches that have been proposed for the dimensionless reporting of irreversibility (that is, in place of N_S).

Extensions to the study of entropy generation in counterflow heat exchangers[14] have been published by Sarangi and Chowdhury[20] and Huang.[29] A study of compact *crossflow heat exchangers* was conducted along similar lines by Baclic and Sekulic.[30] Their study reveals once again the tradeoff between heat transfer and fluid flow irreversibilities, and the remanent (flow imbalance) irreversibility associated purley with the cross-flow arrangement. Basic studies of the thermodynamics of forced convection heat transfer were also undertaken by Dr. Soumerai in Switzerland.[31-33] The relationship between irreversibility minimization and cost minimization was illustrated by Wepfer *et al.* in the problem of deciding the optimum size of a steam pipe and its insulation.[34]

A new and promising direction has been traced in a sequence of studies by Professor Zilberberg.[35-38] He draws attention to the unsteady (often periodic) character of the operation of most power and refrigeration plants and to the irreversibility due solely to this unsteadiness. He calls this effect *dynamic irreversibility*. Problems of plant start-up and shut-down also fall in the domain identified by Professor Zilberberg, as does the basic thermal energy storage problem reviewed in the next section.

The design principle that works at the component and subcomponent level also works at the overall system level. In the realm of heat exchanger design, then, it is worth noting the application of second-law concepts to the optimization of entire *heat exchanger networks*. Studies of this kind have been contributed most recently by Chato and Damianides[39] and Hesselmann.[40]

Finally, we turn our attention to the choice of dimensionless reporting of the calculated irreversibility figure. In most of the examples reviewed until now, the entropy generation rate was nondimensionalized by dividing it through a capacity flowrate, say, $(\dot{m}c_P)_2$ in the case of imbalanced two-stream heat exchangers (Eq. 79). The *entropy generation numbers* that can be defined in this manner (N_S, $N_{S,\Delta T}$, $N_{S,\Delta P_1}$, and so on) are second-law "relatives" of the older concept of number of heat transfer units (N_{tu}), which is used in traditional first-law analyses of heat exchangers. And just like the N_{tu}, the N_S value can vary from 0 all the way to ∞: Whether the calculated N_S represents a high or low entropy generation rate depends on the size of heat exchanger N_S that can be economically tolerated (see the discussion centered on Eq. 83), on the magnitude of the remanent irreversibility, $N_{S,\text{imbalance}}$ (Figure 10), and certainly, on the entropy generation levels shown by the other components that make up the greater system.

In some problems, it is possible to nondimensionalize $\dot{S}_{gen}$ by dividing it through a known entropy generation rate, which is regarded as reference. An example of this kind is the *augmentation entropy generation number* $N_{S,a}$ (Eq. 18).

Another dimensionless measure of heat exchanger irreversibility is the rational (second-law) effectiveness introduced by Bruges[41] and Reistad:[42]

$$\varepsilon_R = \frac{\text{availability (exergy) gained by the cold stream}}{\text{availability (exergy) donated by the warm stream}} = \frac{\dot{m}_C(e_{x,out} - e_{x,in})_C}{\dot{m}_H(e_{x,in} - e_{x,out})_H} \tag{94}$$

This quantity varies monotonically with the entropy generation number N_S:

$$\varepsilon_R = 1 - \frac{T_0\dot{S}_{gen}}{\dot{m}_H(e_{x,in} - e_{x,out})_H} = 1 - \frac{T_0 c_{P,H}}{(e_{x,in} - e_{x,out})_H} N_S \tag{95}$$

where, for the sake of the argument, $N_S = \dot{S}_{gen}/(\dot{m}c_P)_H$, and T_0 is the absolute temperature of the ambient. In the limit of reversible heat exchanger operation (zero ΔT and ΔP's), ε_R is equal to 1. The lowest possible value for ε_R is 0: This occurs in the limit in which the heat exchanger physically disappears. Assuming the pressure drop irreversibility contribution is negligible, Golem and Brzustowski[43] showed ε_R reduces to

$$\varepsilon_R = \pm \frac{(\dot{m}c_P)_C[T_{out} - T_{in} - T_0 \ln(T_{out}/T_{in})]_C}{(\dot{m}c_P)_H[T_{out} - T_{in} - T_0 \ln(T_{out}/T_{in})]_H} \tag{96}$$

where the subscripts in and out refer to the outlets and inlets, respectively, the + sign applies to counterflow, and the − sign to parallel flow. Equation (96) holds for ideal gases and for incompressible liquids with negligible pressure drop. The same authors extended the ε_R concept to the local level, showing that when the longitudinal temperature distributions $T_C(x)$ and $T_H(x)$ are known, one can evaluate locally the destruction of exergy via heat transfer across the stream-to-stream temperature difference.

The newest proposal for the dimensionless reporting of heat exchanger irreversibility is due to Professors Witte and Shamsundar[44] of the University of Houston. Their second-law heat exchanger efficiency is defined as

$$\eta_{W\text{-}S} = 1 - \frac{T_0\dot{S}_{gen}}{\dot{Q}} \tag{97}$$

where $\dot{Q}$ is the total stream-to-stream heat transfer rate,

$$\dot{Q}=\dot{m}_H(h_{in}-h_{out})_H=\dot{m}_C(h_{out}-h_{in})_C \tag{98}$$

The reason for choosing the efficiency expression (Eq. 97) is that while evaluating the thermodynamic imperfection of a real heat exchanger by comparing it with an ideal one that operates reversibly, Witte and Shamsundar regard $\dot{Q}$ as fixed. The $\eta_{W\text{-}S}$ efficiency is related to ε_R and N_S in the following ways:

$$\eta_{W\text{-}S}=1-\frac{T_0 c_{P,H}}{(h_{in}-h_{out})_H}N_S \tag{99}$$

$$\frac{1-\eta_{W\text{-}S}}{1-\varepsilon_R}=\left(\frac{e_{x,in}-e_{x,out}}{h_{in}-h_{out}}\right)_H \tag{100}$$

where N_S was defined again as $\dot{S}_{gen}/(\dot{m}c_P)_H$. If pressure drops are neglected, a visually pleasing alternative to writing $\eta_{W\text{-}S}$ is[44]

$$\eta_{W\text{-}S}=1+\frac{T_0}{\bar{T}_H}-\frac{T_0}{\bar{T}_C} \tag{101}$$

where $\bar{T}_H$ and $\bar{T}_C$ are two average temperatures defined by

$$\bar{T}_{H,C}=\left(\frac{\int_{in}^{out}dh}{\int_{in}^{out}ds}\right)_{H,C} \tag{102}$$

It can be demonstrated that the highest value of the Witte-Shamsundar efficiency is $\eta_{W\text{-}S}=1$ and that it occurs in the limit of reversible operation. The same conclusion is reached by substituting $\varepsilon_R \leqslant 1$ into Eq. (100). Not noted until now is that $\eta_{W\text{-}S}$ can assume *negative* values, and its full range is $-\infty<\eta_{W\text{-}S}\leqslant 1$. A negative $\eta_{W\text{-}S}$ value would characterize a counterflow heat exchanger working at cryogenic temperatures (for example, $T_0=300$ K, $\bar{T}_H=30$ K, $\bar{T}_C=26$ K; hence, $\eta_{W\text{-}S}=-0.54$).

Thermal energy storage

Energy storage versus exergy storage

The growing emphasis placed on energy conservation measures has renewed the interest in thermal energy storage systems,[45] that is, in the type of system whose job is to store temporarily the energy received during a heat transfer interaction. A system like this is capable of providing at a later time a heat transfer interaction of its own. The traditional view in this design area is that a storage unit is efficient when the energy increase experienced during the storage phase approaches the maximum energy increase the unit is capable of. For example, a batch of incompressible liquid of mass m, constant specific heat c, and initial temperature T_0 can experience a maximum energy increase equal to $mc(T_\infty-T_0)$ if the temperature of the heat source that heats the batch is T_∞. In the traditional sense, the goodness of this unit can be quantized in terms of a first-law efficiency ratio

$$\eta_I=\frac{\text{actual energy increase}}{\text{maximum energy increase}}=\frac{mc(T-T_0)}{mc(T_\infty-T_0)} \tag{103}$$

where T is the temperature of the batch of liquid at the end of the storage process.

The first-law efficiency η_I can have values greater than 0 and less than 1. The desirable limit $\eta_I\to 1$ is approached through a number of design decisions, for example, by increasing the size of the heat exchanger placed between the liquid batch and the heat source and by increasing the time of thermal communication between heat source and storage material.

The traditional view was challenged on thermodynamic grounds in 1978.[46] It seemed that if the upgrading of power system performance depends on the designer's ability to eliminate or, at least, reduce irreversibilities, the real purpose of using storage systems in the power-system area must also be the reduction of irreversibility. And if the reduction of irreversibility amounts to an exergy flow that is more nearly "conserved' as it descends through the power plant, the mission of the storage device is to temporarily store *exergy*, not energy. This new viewpoint has developed into a distinct subfield in the thermal design of energy storage systems, as exemplified by the recent work of Krane,[47,48] Mathiprakasam and Beeson,[49] and Taylor.[50]

The optimum duration of the storage process

The destruction of exergy in a storage system and the opportunity for minimizing this destruction become apparent if we examine the first phase (storage phase) in the operation of the system sketched in Figure 12. (An extensive treatment of this example is given in ref. 46, as well as in ref. 2, ch. 8.) The storage system (the left side of the figure) contains the batch of incompressible liquid (m, c) alluded to earlier. The liquid is held in an insulated vessel. The hot gas stream $\dot{m}$ enters the system through one port and is gradually cooled as it flows through a heat exchanger immersed in the liquid bath. The spent gas is discharged directly into the atmosphere. As time passes, the bath temperature T and the gas outlet temperature T_{out} approach the hot gas inlet temperature, T_∞.

Focusing on the irreversibility of the energy storage process, we see in Figure 12 that the irreversibility is divided between two distinct parts of the apparatus. First, there is the finite-ΔT irreversibility associated with the heat transfer between the hot gaseous stream and the cold liquid bath. Second, the stream exhausted into the atmosphere is eventually cooled down to T_0, again by heat transfer across a finite ΔT. Neglected in the present model is the irreversibility due to the pressure drop across the heat exchanger traveled by the stream $\dot{m}$.

The combined effect of the competing irreversibilities noted in Figure 12 is a characteristic of all sensible-heat energy storage systems. Because of it, only a small fraction of the exergy content of the hot stream can ever be stored in the liquid bath. To see this, consider the instantaneous rate of entropy generation in the overall system delineated in Figure 12:

$$\dot{S}_{gen}=\dot{m}c_P\ln\frac{T_0}{T_\infty}+\frac{\dot{Q}_0}{T_0}+\frac{d}{dt}(mc\ln T) \tag{104}$$

where $\dot{Q}_0=\dot{m}c_P(T_{out}-T_0)$. More important than $\dot{S}_{gen}$ is the entropy generated during the entire "charging" time interval 0–t, which can be put in dimensionless form as[46]

$$\frac{1}{mc}\int_0^t \dot{S}_{gen}dt=\theta\left(\ln\frac{T_0}{T_\infty}+\tau\right)+\ln(1+\tau\eta_I)-\tau\eta_I \tag{105}$$

where η_I is given by Eq. (103), and

$$\tau=\frac{T_\infty-T_0}{T_0},\qquad \theta=\frac{\dot{m}c_P}{mc}t \tag{106}$$

Multiplied by T_0, the entropy generation integral $\int_0^t \dot{S}_{gen}dt$ calculated above represents the bite taken by irreversibilities out of the total exergy supply brought into the system by the hot stream. On this basis, we define the entropy generation number

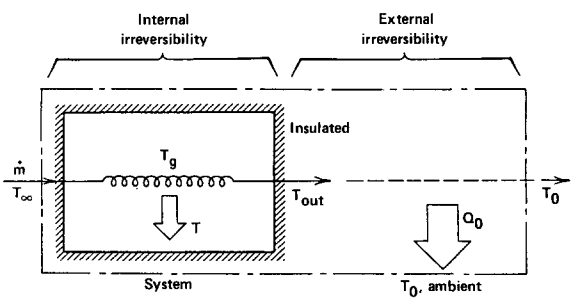

Figure 12 Two sources of irreversibility in a batch-heating process

N_S as the ratio of the lost exergy divided by the total energy invested during the time interval 0–t,

$$N_S(\theta, \tau, N_{tu}) = \frac{T_0}{E_x}\int_0^t \dot{S}_{gen}dt = 1 - \frac{\tau\eta_I - \ln(1+\tau\eta_I)}{\theta[\tau - \ln(1+\tau)]} \tag{107}$$

This particular entropy generation number takes values in the range 0–1, the $N_S = 0$ limit representing the elusive case of reversible operation. Worth noting is the relation $N_S = 1 - \eta_{II}$, where η_{II} is the second-law efficiency of the installation during the charging process.

Charts of the $N_S(\theta, \tau, N_{tu})$ surface show[2,46] that N_S decreases steadily as the heat exchanger size (N_{tu}) increases. This effect is expected; in fact, it matches the N_{tu}-related conclusion drawn based on first-law arguments (Eq. 103). Less expected is that N_S goes through a minimum as the dimensionless time θ increases. For example, the optimum time for minimum N_S can be calculated analytically in the limit $\tau \ll 1$, where Eq. (107) reduces to

$$N_S = 1 - \frac{1}{\theta}[1 - \exp(-y\theta)]^2 \tag{108}$$

and

$$y = 1 - \exp(-N_{tu}), \qquad N_{tu} = \frac{\bar{h}_b A_b}{\dot{m}c_P} \tag{109}$$

The solution of the equation $\partial N_S/\partial\theta = 0$ is

$$\theta_{opt} = 1.256[1 - \exp(-N_{tu})]^{-1} \tag{110}$$

that is, for the common range of N_{tu} values (1–10), the optimum dimensionless charging time is consistently *a number of order 1*. This conclusion continues to hold as τ takes values greater than 1.[46]

Away from the optimum charging time illustrated above (when $\theta \to 0$ or $\theta \to \infty$) the entropy generation number N_S approaches unity. In the short-time limit ($\theta \ll \theta_{opt}$), the entire exergy content of the hot stream is destroyed by heat transfer to the liquid bath, which was initially at atmospheric temperature, T_0. In the long-time limit ($\theta \gg \theta_{opt}$), the external irreversibility takes over: In this limit, the used stream exits the heat exchanger as hot as it enters ($T_{out} = T_\infty$), and because of this, its exergy content is destroyed entirely by the heat transfer (or mixing) with the T_0 atmosphere. The first-law rule of thumb of increasing the time of communication between heat source and storage material (Eq. 103) is counterproductive from the viewpoint of avoiding the destruction of exergy.

The optimum size of the heat exchanger

Continuing the example constructed based on Figure 12, we inquire into the effect of heat exchanger N_{tu} on the overall irreversibility of the energy storage phase. In the study of heat exchanger irreversibilities, we learned to expect a tradeoff with respect to N_{tu}, as a result of the competition between heat transfer and fluid flow irreversibilities. The same tradeoff appears in the design of the heat exchanger of Figure 12 as soon as we take into account the pressure drop (ΔP) between the stream inlet and outlet. It has been shown that when the pressure drop entropy generation is not neglected, the N_S expression (Eq. 107) contains an additional term,[46] now labeled $N_{S,\Delta P}$:

$$N_S = \underbrace{\frac{(R/c_P)fg^2N_{tu}}{[\tau - \ln(1+\tau)]\mathrm{St}}}_{N_{S,\Delta P}} + \underbrace{1 - \frac{\tau\eta_I - \ln(1+\tau\eta_I)}{\theta[\tau - \ln(1+\tau)]}}_{N_{S,\Delta T}\text{ or }N_S\text{ of Eq. (107)}} \tag{107'}$$

In this additional term, f and St represent the friction factor and Stanton number on the gas side of the heat exchanger. It is also being assumed that the overall N_{tu}, defined in Eq. (109), is practically equal to the number of heat transfer units for the gas side of the heat exchanger. Finally, the dimensionless mass velocity g is defined according to Eq. (51). In the case where the $N_{S,\Delta T}$ part has already been minimized with respect to θ, the optimum N_{tu} that minimizes the whole N_S expression (Eq. 107′) is [46]

$$N_{tu,opt} = \ln\left[\frac{\tau^2\eta_I(1-\eta_I)}{1+\tau\eta_I}\right] - \ln\left(\frac{Rg^2f}{c_P\mathrm{St}}\right) \tag{111}$$

In the optimum charging time regime, the first term on the right-hand side depends only on τ. Therefore, the optimum number of heat transfer units depends only on τ and the group $(Rg^2f/c_P\mathrm{St})$. Since for most heat exchanger surface types, the ratio f/St is only a weak function of Reynolds number, the optimum N_{tu} depends primarily on τ and g.

Storage followed by removal of exergy

The two optima analyzed until now rule the design of more complex processes executed by energy storage systems. A necessary step in the direction of completing the thermodynamic treatment of these systems was taken by Professor Robert J. Krane of the University of Tennessee, who considered the cyclical operation of the device.[48] Figure 13 shows the schematic evolution of the liquid bath temperature during the storage phase and the exergy removal phase that follows immediately. The liquid temperature varies periodically without ever reaching the limiting temperature levels T_0 and T_∞.

Figure 14 provides insight into the irreversibility composition of the storage and removal cycle. The only parameter that varies in this example is the duration of the storage part of the cycle, θ. The storage part is accompanied by the irreversibilities discussed already, namely, the contributions due to heat exchanger ΔT, heat exchanger ΔP, and the dumping of the used stream into the atmosphere. The exergy removal part of the cycle is plagued by irreversibilities due only to heat exchanger ΔT and ΔP. The gas stream $\dot{m}_r$ heated by the liquid pool during the removal phase—the fruit of the entire scheme—is delivered to a power cycle that can use its exergy content. In Figure 14, the two pressure drop effects (during storage and removal) are shown added up under the same curve.

Krane's Figure 14 begins to show the importance of fine-tuning the timing of the storage and removal phases to minimize the cycle-integrated destruction of the original exergy content of the hot stream ($\dot{m}$, T_∞). The optimization of the whole cycle and the gas-liquid heat exchanger can be accomplished numerically by minimizing the total N_S with respect to the charging interval (θ) and the heat exchanger size (N_{tu}). For the design case illustrated in Figure 14, Krane obtained

$\theta_{opt} = 0.863$, optimum charging (storage) interval
$N_{tu,opt} = 5.53$, optimum number of heat transfer units
$N_{S,min} = 0.734$, minimum entropy generation number, that is, $\eta_{II} = 0.266$ (under the same conditions, $\eta_I = 0.577$)

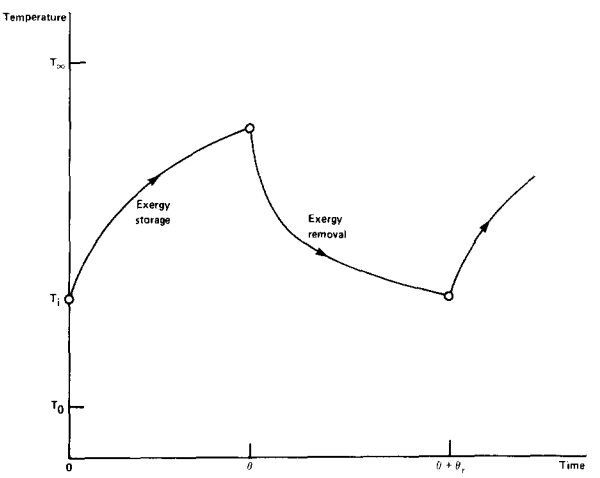

Figure 13 The batch-system temperature evolution during a complete exergy storage and exergy removal cycle

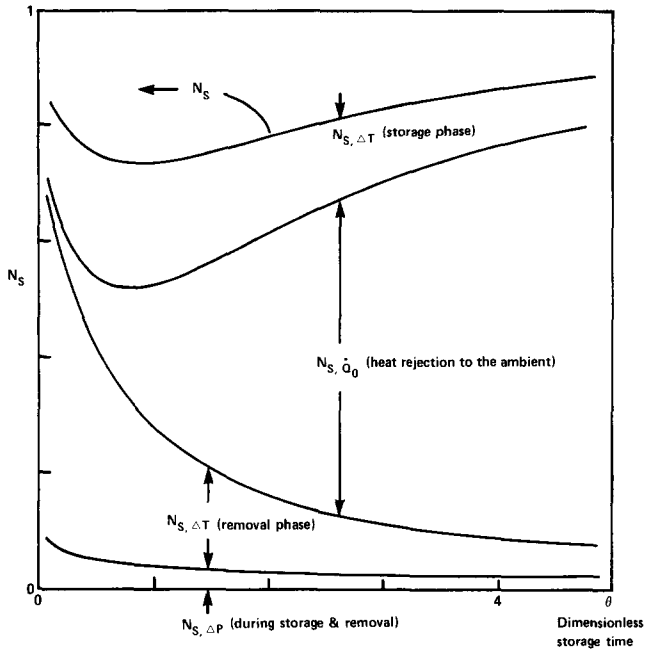

Figure 14 The effect of charging time on the irreversibilities of the storage and removal cycle

The inlet temperature of the stream of cold gas $\dot{m}_r$ was assumed to be the same as T_0. The dimensionless time interval of the exergy removal part of this cycle, θ_r, was found to be equal to 1.83. Other parameters held fixed during this optimization example are

$$\frac{\dot{m}_r}{\dot{m}}=1, \qquad g=0.0354, \qquad \frac{T_i}{T_0}=1.1,$$
$$\text{Pr}=0.71, \qquad \frac{R}{c_P}=0.286 \tag{112}$$

The dimensionless pressure drop ratios ($\Delta P/P$) during the storage and removal phases were 0.021 and 0.01, respectively.

The conclusions reached during the study of the storage phase alone are reinforced by Krane's study of the complete storage and removal cycle. The optimum storage time interval, for example, is such that in dimensionless terms it emerges once more as a number of order 1. There exists again an optimum number of heat transfer units for the gas–liquid heat exchanger. The minimum N_S values revealed by Krane's study are generally greater than the values encountered in the study of the storage phase alone.[46] This effect is due to the irreversibilities contributed by the exergy removal phase of the cycle.

Figure 14 makes the point that the task of perfecting the thermodynamic performance of storage system hinges on the ability to minimize the heat transfer across three temperature gaps, namely, the ΔT between gas and liquid during both storage and removal and the ΔT between the stream exhausted at the end of the storage phase. These ΔT's can be reduced by bringing the inlet temperature of the stream closer to the temperature of the liquid bath and by keeping the exhaust temperature T_{out} as close to T_0 as possible. This proposal can be executed in strikingly simple fashion by using a large number of storage units positioned in series. During the storage phase, the stream exhausted by the i unit becomes the exergy source stream of the (i + 1) unit, and so on.[2] That is, the stream exhausted by the i unit does not reject heat to T_0 but to a higher temperature—the temperature of the (i + 1) unit.

In the series arrangement described above, the temperature of the storage units decreases monotonically in the direction of flow. During the exergy recovery phase, the cold stream is led in the opposite direction, that is, the direction of increasing temperature, or in counterflow relative to the stream used during the storage phase. The ΔT's between the stream and storage material and the exhaust stream and ambient are considerably smaller in this arrangement. This proposal was investigated in great detail by Taylor[50] based on a solid "distributed storage element" model, in which the storage material temperature varied continuously along the stream. Taylor shows, among other things, that the longitudinal conduction of heat through the storage material during the periodic operation of the heat exchanger can have a major impact on the overall irreversibility of the installation. The overall irreversibility figure N_S is again a strong function of the time interval required by the storage part of the cycle: The identification of the optimum storage time interval is critical. The overall N_S is affected also by the geometric aspect ratio of the storage material. The numerical examples documented in Taylor's study reveal N_S values that cover the range 0.2–0.8. This range compares favorably with the 0.7–0.9 range covered by the N_S results obtained for a single sensible-heat element during complete storage and removal cycles.[48]

The cyclical storage and removal of exergy from a continuous one-dimensional stretch of storage material was studied also by Mathiprakasam and Beeson.[49] One interesting effect illustrated by these authors is that of the direction of flow during the removal phase. They found that the second-law efficiency $(1-N_S)$ is always lower if the exergy-removal stream flows in the same direction as the original exergy-supply stream (that is, in parallel), lower than in the counterflow arrangement discussed in the preceding paragraph. The relative inferiority of the parallel flow arrangement was also illustrated by Taylor.[50]

Closely related to the continuous one-dimensional storage scheme with periodic counterflow circulation is the class of periodic heat exchangers recognized as "regenerators." The design of this type of heat exchanger was approached on the basis of entropy generation minimization by San, Worek, and Lavan.[51] Their model consists of two-dimensional parallel-plate channels sandwiched between slabs of energy storage material. The longitudinal conduction of heat through the storage material is neglected. An important difference between this regenerator model and the continuous storage system analyzed by Taylor[50] is that in the case of the regenerator the stream exhausted during the storage phase is not dumped into the atmosphere. That stream and the exergy still left in it are considered usable. Therefore, the total entropy generation figure of one full cycle in the operation of the regenerator is due to four contributions, namely, the ΔT- and ΔP-inspired irreversibilities of the storage part and the removal part of the cycle.

Worthy of mention in this section is the thermodynamic investigation of another simple device for temporary exergy storage, one where the heating during the storage phase is provided by an electrical resistance (Joulean heating).[47] Three sources of irreversibilities are identified in the operation of this device: the electrical resistive heating itself, the heat transfer across the finite ΔT between the storage material and the stream used during the exergy removal phase, and the flow with pressure drop through the heat exchanger built between the stream and the storage material. The entropy generation numbers (N_S) revealed by this study fall in the range 0.6–0.8.

Heating and cooling subject to time constraint

Related to the lumped system model sketched in Figure 12 is the metallurgical problem of heating an object to a prescribed temperature level[52,53] and the cooldown problem of cryogenics, where large-scale superconducting windings must first be cooled to liquid helium temperature before they can be operational.[54] For the sake of concreteness, consider the cooldown process by which the lumped system (m, c) is cooled from an original temperature T_i to a lower temperature T_f by a single-phase stream $(\dot{m}c_P)$ whose temperature T_L is lower than T_f. The expensive commodity in this operation is the total amount of

cold gas used to do the job:

$$m_{0-t_c}=\int_0^{t_c}\dot{m}(t)dt \tag{113}$$

where t_c is the duration of the cooldown process. The total mass m_{0-t_c} is an expensive commodity because it is directly proportional to its exergy content and to the actual refrigerator power required to produce it.

When the cooldown time is fixed by logistic and economic considerations, there exists an optimum cold-gas flowrate history $\dot{m}(t)$ that minimizes the overall expenditure of cryogen, m_{0-t_c}. (The details of the model and analysis that produces this result[52,54] are given in ref. 2, pp. 166–169.) The optimum flowrate history is

$$\dot{m}_{opt}=\left[\frac{\bar{h}_b(T)A_b}{C^*c_P(T)}\right]^{1/2} \tag{114}$$

where C^* is a constant that depends on the overall cooldown time t_c.

In conclusion, the optimum flowrate is time-independent only in those cases where $\bar{h}_b$ and c_P do not vary as the temperature of the ensemble decreases. In general, however, the overall heat transfer coefficient varies with the temperature: From the optimum cooldown regime (Eq. 114), we learn that during periods of poor heat transfer (low $\bar{h}_b$), the coolant flowrate must be decreased. If during the same cooldown run, the specific heat of the cold gas (c_P) increases as T decreases (as in N_2 gas at constant P, for example), the coolant flowrate must again decrease. The optimum flowrate $\dot{m}_{opt}(t)$ depends on T indirectly, via $\bar{h}_b(T)$ and $c_P(T)$.

Mass exchangers

The thermodynamic optima identified in the study of heat exchangers and related heat transfer applications surface again in the thermodynamic design of mass transfer devices. The work on the minimization of entropy generation in the mass transfer domain is even newer than what has been accomplished in heat transfer; therefore, one of our objectives in this section is to place in perspective the newly emerging subfield of mass-transfer thermodynamic design.

Convective mass transfer

As an analogy to the most basic problem of heat exchanger irreversibility at the flow-passage level (investigated in refs. 2 and 3), the competition between fluid flow and mass transfer irreversibilities in a mass exchanger was studied by San, Worek, and Lavan.[55] The general expression for the rate of entropy generation in a flow field with both heat and mass transfer and without body force and chemical reaction effects is[56]

$$s'''_{gen}=\underbrace{-\frac{1}{T}\sum_i \mathbf{j}_i\cdot\nabla\mu_i}_{\text{mass diffusion}}+\underbrace{\frac{\mu}{T}\Phi}_{\text{fluid friction}}-\underbrace{\frac{1}{T^2}\mathbf{q}\cdot\nabla T}_{\text{thermal diffusion}}-\underbrace{\frac{1}{T}\sum_i \bar{s}_i\mathbf{j}_i\cdot\nabla T}_{\text{coupling between thermal diffusion and mass diffusion}} \tag{115}$$

where $\mathbf{j}_i$ is the mass diffusion flux vector of the i species, and $\bar{s}_i$ the partial molal entropy of the species

$$\bar{s}_i=-\left(\frac{\partial\mu_i}{\partial T}\right)_{P,N_k},\qquad (k\neq i) \tag{116}$$

Worth noting is Eq. (28) as a special case of Eq. (115), namely, the limiting case of zero mass transfer. In the *zero heat transfer limit*, on the other hand, we retain only the first two terms on the right-hand side of Eq. (115) and concentrate on the interplay between fluid friction and mass diffusion irreversibilities. Regarding the chemical potential gradient that appears in the mass diffusion term, we recall from the study of convective mass transfer (ref. 4, ch. 9) that the mass transfer part of the problem is usually described in terms of species concentration distributions, C_i [moles of i/m^3], not in terms of chemical potential. Useful then is the invocation of the ideal gas mixture model,

$$\mu_i(T,P_i)=\mu_i(T,P_0)+\bar{R}T\ln\frac{P_i}{P_0} \tag{117}$$

where the partial pressure of i in the mixture of pressure P_0 and temperature T is

$$P_i=C_i\bar{R}T \tag{118}$$

If, in addition, we invoke Fick's law of mass diffusion,

$$\mathbf{j}_i=-D_i\cdot\nabla C_i \tag{119}$$

the entropy generation expression (Eq. 115) reduces to[55]

$$s'''_{gen}=\bar{R}\sum_i\frac{D_i}{C_i}(\nabla C_i)^2+\frac{\mu}{T}\Phi \tag{120}$$

This two-term expression is the analog of Eq. (30) of convective heat transfer. For example, in the case of two-dimensional flow (v_x, v_y) through the space (x, y) in which only the i species diffuses, Eq. (120) reads

$$s'''_{gen}=\bar{R}\frac{D_i}{C_i}\left[\left(\frac{\partial C_i}{\partial x}\right)^2+\left(\frac{\partial C_i}{\partial y}\right)^2\right]+\frac{\mu}{T}\left\{2\left[\left(\frac{\partial v_x}{\partial x}\right)^2+\left(\frac{\partial v_y}{\partial y}\right)^2\right]+\left(\frac{\partial v_x}{\partial y}+\frac{\partial v_y}{\partial x}\right)^2\right\} \tag{121}$$

Both terms on the right-hand side of Eq. (121) are positive, indicating the permanent collaboration between fluid friction and mass diffusion in determining the irreversibility rate at each point in the flow field. The similarity between Eqs. (121) and (31) of convective heat transfer assures us that the thermodynamic tradeoffs discovered in the field of heat transfer and thermal design exist also in the design of mass transfer devices. San, Worek, and Lavan[55] demonstrated this by considering the design of a two-dimensional mass exchanger in which the fluid mixture flows through a parallel plate channel with imposed uniform mass flux of i normal to the flow. They also assumed the "small diffusion rate" limit, in which the velocity profile in the channel cross section is not affected by the species that diffuses in the direction normal to the flow. Minimizing the entropy generation rate integrated over the channel cross section, San, Worek, and Lavan[55] developed a complete sizing procedure for the plate-to-plate spacing of the channel, for both laminar and turbulent flow. Their paper and results are highly recommended.

Simultaneous mass and heat transfer by convection

The problem of entropy generation minimization in combined convective heat and mass transfer was considered in a subsequent paper by San, Worek, and Lavan.[57] As indicated by Eq. (115), in this case, the irreversibility is due to four distinct effects: pure mass diffusion, fluid friction, pure thermal diffusion, and the couping between thermal diffusion and mass diffusion. After involving one more time the Fick and Fourier laws of diffusion, the local entropy generation rate (Eq. 115) can be written as

$$s'''_{gen}=\bar{R}\sum_i\frac{D_i}{C_i}(\nabla C_i)^2+\frac{\mu}{T}\Phi+\frac{k}{T^2}(\nabla T)^2+\frac{1}{T}\sum_i\bar{s}_iD_i(\nabla C_i)\cdot(\nabla T) \tag{122}$$

Whether all four terms are important in the final s'''_{gen} figure depends, of course, on the particular convection problem being investigated. For example, consider the heat and mass transfer to fully developed laminar flow through a parallel-plate channel of size (spacing) D, and let ΔC_i and ΔT represent the scales of the

wall—mean concentration and temperature differences. Taking $\bar{R}$ as the scale of $\bar{s}_i$ in Eq. (122), the importance of the fourth term (coupling) relative to the first term (mass diffusion) is measured by the ratio

$$\frac{\text{heat and mass transfer coupling}}{\text{pure mass diffusion}} \sim \frac{\Delta T/T}{\Delta C_i/C_i} \tag{123}$$

We see here the emergence of another family of dimensionless groups for second-law analysis, namely, the dimensionless ratios $(\Delta C/C)_i$. In the description of mass tranfer irreversibility, these ratios play the same role as the $\Delta T/T$ ratio in heat transfer and the $\Delta P/P$ ratios in duct flow with friction.

The complete four-term entropy generation rate expression (Eq. 122) was used by San, Worek, and Lavan[57] for determining the optimum spacing (D) of a parallel-plate heat and mass exchanger with uniform heat and mass fluxes. They showed that the thermodynamic optimum is due to the fact that the fluid friction term varies as D^{-3}, whereas the remaining terms are directly proportional to D.

Of the thermodynamic design work devoted to mass transfer processes, a substantial part deals with the optimization of drying and moistening processes (for example, Sieniutycz[58-61]), the dehumidification of air,[62] and the dessicant cooling systems.[63,64] A general framework for the calculation of mass transfer irreversibility in chemical separation systems was constructed by Moore and Wepfer.[65]

Convective heat and mass transfer through a saturated porous medium

Considering the step-by-step evolution from convective heat transfer (Eq. 30) to combined heat, mass, and fluid flow (Eq. 122), this is an opportunity to generalize the entropy generation rate formula for convection through a saturated porous medium (first stated in ref. 4, p. 355). Writing term-by-term the porous-medium equivalent of Eq. (122),

$$s'''_{\text{gen}} = \bar{R}\sum_i \frac{D_{\text{pm},i}}{C_{\text{pm},i}}(\nabla C_{\text{pm},i})^2 + \frac{\mu}{KT}(\mathbf{v}_{\text{pm}})^2 + \frac{k_{\text{pm}}}{T^2}(\nabla T)^2 + \frac{1}{T}\sum_i \bar{s}_{\text{pm},i} D_{\text{pm},i}(\nabla C_{\text{pm},i})\cdot(\nabla T) \tag{124}$$

we note the special form of the fluid friction contribution (the second term), in which $\mathbf{v}_{\text{pm}}$ is the volume-averaged velocity vector through the mixture-saturated porous medium. The second term owes its compact form to the Darcy flow model, K being the permeability constant of the medium. The saturated porous medium is further modeled as homogeneous and isotropic with an effective thermal conductivity k_{pm}. The solid matrix is locally in thermal equilibrium with the fluid that seeps through it. The concentration $C_{\text{pm},i}$ is a volume-averaged quantity also, since it represents the number moles of i per cubic meter of porous medium saturated with fluid. The partial molal entropy $s_{\text{pm},i}$ is also a volume-averaged quantity. The coefficient $D_{\text{pm},i}$ is the mass diffusivity of the i species through the porous medium saturated with the fluid mixture i belongs to.

The thermodynamic design developements reviewed in this paper are only a part of the modern look of engineering thermodynamics. The latter forms the subject of a new graduate textbook.[66]

Acknowledgements

The author's research during 1986 was supported by Duke University, the Lord Foundation of North Carolina, the Electric Power Research Institute, and the National Science Foundation.

References

1 Bejan, A. Second-law analysis in heat transfer and thermal design. *Adv. Heat Transfer*, 1982, **15**, 1–58

2 Bejan, A. *Entropy Generation through Heat and Fluid Flow*. Wiley, New York, 1982, ch. 5–9

3 Bejan, A. General criterion for rating heat-exchanger performance. *Int. J. Heat and Mass Transfer*, 1978, **21**, 655–658

4 Bejan, A. *Convection Heat Transfer*. Wiley, New York, 1984, ch. 7

5 Bejan, A. Second law analysis in heat transfer. *Energy*, 1980, **5**, 721–732

6 Kotas, T. J. and Shakir, A. M. Exergy analysis of a heat transfer process at sub-environmental temperature. *Computer-Aided Engineering of Energy Systems*, ed. Gaggioli, R. A., ASME, AES, 1986, **2–3**, 87–92

7 Bejan, A. and Pfister, P. A., Jr. Evaluation of heat transfer augmentation techniques based on their impact on entropy generation. *Lett. Heat and Mass Transfer*, 1980, **7**, 97–106

8 Ouellette, W. R. and Bejan, A. Conservation of available work (exergy) by using promoters of swirl flow. *Energy*, 1980, **5**, 587–596

9 Perez-Blanco, H. Irreversibility in heat transfer enhancement. *Second Law Aspects of Thermal Design*, ed. Bejan, A. and Reid, R. L., ASME, HTD, 1984, **33**, 19–26

10 Poulikakos, D. and Bejan, A. Fin geometry for minimum entropy generation in forced convection. *J. Heat Transfer*, 1982, **104**, 616–623

11 Poulikakos, D. Fin geometry for minimum entropy generation. M.S. thesis, Department of Mechanical Engineering, University of Colorado, Boulder, December 1980

12 Bejan, A. A study of entropy generation in fundamental convective heat transfer. *J. Heat Transfer*, 1979, **101**, 718–725

13 Moody, F. J. Second law thinking—example applications in reactor and containment technology. *Second Law Aspects of Thermal Design*, ed. Bejan, A. and Reid, R. L., ASME, HTD, 1984, **33**, 1–9

14 Bejan, A. The concept of irreversibility in heat exchanger design: counterflow heat exchangers for gas-to-gas applications. *J. Heat Transfer*, 1977, **99**, 374–380

15 Rohsenow, W. M. and Choi, H. Y. *Heat, Mass and Momentum Transfer*. Prentice-Hall, Englewood Cliffs, N.J., 1961, 315

16 Bejan, A. *Solutions Manual for Entropy Generation through Heat and Fluid Flow*. Wiley, New York, 1984, problem 7.2, 36–37. This manual is available from the author

17 Sekulic, D. P. and Herman, C. V. One approach to irreversibility minimization in compact crossflow heat exchanger design. *Comm. Heat and Mass Transfer*, 1986, **13**, 23–32

18 Kays, W. M. and London, A. L. *Compact Heat Exchangers*. McGraw-Hill, New York, 1964

19 Tribus, M. Private communication, course notes Thermo-economics, Massachusetts Institute of Technology, Cambridge, Massachusetts, September 1978

20 Sarangi, S. and Chowdhury, K. On the generation of entropy in a counterflow heat exchanger. *Cryogenics*, 1982, **22**, 63–65

21 Sekulic, D. P. and Baclic, B. S. Enthalpy exchange irreversibility. *Publications of the Faculty of Technical Sciences*, University of Novi Sad, Yugoslavia, 1984, No. 15, 113–123

22 da Costa, C. E. S. M. and Saboya, F. E. M. Second law analysis for parallel flow and counterflow heat exchangers. Proceedings of the Eighth Brazilian Congress of Mechanical Engineering, VIII COBEM, Sao Jose dos Campos, S.P., Brazil, December 1985, 185–187

23 Sekulic, D. P. Unequally sized passes in two-pass crossflow heat exchangers: a note on the thermodynamic approach to the analysis. *Publications of the Faculty of Technical Sciences*, University of Novi Sad, Yugoslavia, 1985/1986, No. 16

24 Sekulic, D. P. Entropy generation in a heat exchanger. *Heat Transfer Eng.*, 1986, **7**(1–2), 83–88

25 Bejan, A. Second-law aspects of heat transfer engineering. Keynote Address to the Third Multi-Phase Flow and Heat Transfer Symposium/Workshop, Miami Beach, Florida, April 18–20, 1983; published in *Multi-Phase Flow and Heat Transfer III*, ed. Veziroglu, T. N. and Bergles, A. E., Elsevier, Amsterdam, 1984, **1A**, 1–22

26 London, A. L. and Shah, R. K. Costs of irreversibilities in heat exchanger design. *Heat Transfer Eng.*, 1983, **4**(2), 59–73

27 Zubair, S. M., Kadaba, P. V. and Evans, R. B. Design and optimization of two-phase heat exchangers. *Two-Phase Heat Exchanger Symposium*, ed. Pearson, J. T. and Kitto, Jr., J. B., ASME, HTD, 1985, **44**; published as Zubair, S. M., Kadaba, P. V. and Evans, R. B. Second law based thermoeconomic optimization of two-phase heat exchangers, *J. Heat Transfer*, 1987, **109**, 287–294

28 London, A. L. Economics and the second law: an engineering view and methodology. *Int. J. Heat and Mass Transfer*, 1982, **25**, 743–751

29 Huang, S. Y. The heat exchanger for capturing energy from waste heat (ORC Technology). *ORC-HP-Technology*, VDI Berichte 539, VDI Verlag, Düsseldorf, 1984, 623–629

30 Baclic, B. and Sekulic, D. A crossflow compact heat exchanger of minimum irreversibility (in Serbo-Croatian). *Termotechnika*, 1978, **4**, 34–42

31 Soumerai, H. P. Second law thermodynamic treatment of heat exchangers. *Second Law Aspects of Thermal Design*, ed. Bejan, A. and Reid, R. L., ASME, HTD, 1984, **33**, 11–18

32 Soumerai, H. P. Thermodynamic considerations on a "mirror image" concept—forced convection single-phase tube flow applications. ASME Paper No. 85-WA/HT-18, Presented at the Winter Annual Meeting, Miami Beach, Florida, November 17–21, 1985

33 Soumerai, H. P. Thermodynamic aspects of adiabatic and diabatic tube flow regime transitions—single-phase fluids. Paper No. AIAA-86-1364, Presented at the AIAA/ASME 4th Joint Thermophysics and Heat Transfer Conference, Boston, Massachusetts, June 2–4, 1986

34 Wepfer, W. J., Gaggioli, R. A. and Obert, E. F. Economic sizing of stream piping and insulation. *J. Eng. Ind.*, 1979, **101**, 427–433

35 Zilberberg, Y. M. On dynamic irreversibilities. *Energy*, 1984, **9**, 1005–1007

36 Zilberberg, Y. M. Impact of heat transfer dynamics on the second law analysis of thermodynamic cycles. *Second Law Aspects of Thermal Design*, ed. Bejan, A. and Reid, R. L., ASME, HTD, 1984, **33**, 39–43

37 Zilberberg, Y. M. Dynamic irreversibilities and their impact on energy efficiency of refrigeration/heat-pump thermodynamic cycles. *CLIMA 2000*, ed. Fanger, P. O., Heating, Ventilating and Air-Conditioning Systems, VVS Kongres-VVS Messe, Copenhagen, 1985, **6**, 77–85

38 Zilberberg, Y. M. Dynamic exergy destruction of statically-reversible heat-transfer processes. ASME Paper No. 85-WA/HT-21, Presented at the Winter Annual Meeting, Miami Beach, Florida, November 17–21, 1985

39 Chato, J. C. and Damianides, C. Second-law-based optimization of heat exchanger networks using load curves. *Int. J. Heat and Mass Transfer*, 1986, **29**, 1079–1086

40 Hesselmann, K. Optimization of heat exchanger networks. *Second Law Aspects of Thermal Design*, ed. Bejan, A. and Reid, R. L., ASME, HTD, 1984, **33**, 95–99

41 Bruges, E. A. *Available Energy and the Second Law Analysis*. Butterworths, London, 1959, 62

42 Reistad, G. M. Availability: concepts and applications. Ph.D. thesis, University of Wisconsin, Madison, 1970

43 Golem, P. J. and Brzustowski, T. A. Second-law analysis of energy processes. Part II. The performance of simple heat exchangers. *Trans. Can. Soc. Mech. Eng.*, 1976–1977, **4**, 219–226

44 Witte, L. C. and Shamsundar, N. A thermodynamic efficiency concept for heat exchange devices. *J. Eng. Power*, 1983, **105**, 199–203

45 Schmidt, F. W. and Willmott, A. J. *Thermal Energy Storage and Regeneration*. Hemisphere, Washington, D.C., 1981

46 Bejan, A. Two thermodynamic optima in the design of sensible heat units for energy storage. *J. Heat Transfer*, 1978, **100**, 708–712

47 Krane, R. J. A second law analysis of a thermal energy storage system with Joulean heating of the storage element. ASME Paper 85-WA/HT-19, Winter Annual Meeting, Miami Beach, Florida, November 17–21, 1985

48 Krane, R. J. A second law analysis of the optimum design and operation of thermal energy storage systems. *Int. J. Heat and Mass Transfer*, 1987, **30**, 43–57

49 Mathiprakasam, B. and Beeson, J. Second law analysis of thermal energy storage devices. *Proceedings of the AIChE Symposium Series*, National Heat Transfer Conference, Seattle, Washington, 1983

50 Taylor, M. J. Second law optimization of a sensible heat thermal energy storage system with a distributed storage element. M.S. thesis, Department of Mechanical and Aerospace Engineering, The University of Tennessee, Knoxville, June 1986

51 San, J. Y., Worek, W. M. and Lavan, Z. Second-law analysis of a two-dimensional regenerator. *Energy*, 1987, **12**, 485–496

52 Geskin, E. S. Second law analysis of fuel consumption in furnaces. *Energy*, 1980, **5**, 949–954

53 Geskin, E. S. Assessment of Energy Use in Material Heating. *Computer-Aided Engineering of Energy Systems*, ed. Gaggioli, R. A., ASME, AES, 1986, **2**(2), 107–112

54 Bejan, A. and Schultz, W. Optimum flowrate history for cooldown and energy storage processes. *Int. J. Heat and Mass Transfer*, 1982, **25**, 1087–1092

55 San, J. Y., Worek, W. M. and Lavan, Z. Entropy generation in convective heat transfer and isothermal convective mass transfer. *J. Heat Transfer*, 1987, **109**, 647–652

56 Hirschfelder, J. O., Curtiss, C. F. and Bird, R. B. *Molecular Theory of Gases and Liquids*. Wiley, New York, 1954

57 San, J. Y., Worek, W. M. and Lavan, Z. Entropy generation in combined heat and mass transfer. *Int. J. Heat and Mass Transfer*, 1987, **30**, 1359–1369

58 Sieniutycz, S. The thermodynamic approach to fluidized drying and moistening optimization. *AIChE Journal*, 1973, **19**(2), 277–285

59 Sieniutycz, S. A synthesis of mathematical models and optimization algorithms of invariant imbedding type for a class of adiabatic drying processes with granular solid suspension. *Chem. Eng. Sci.*, 1982, **37**(10), 1557–1568

60 Sieniutycz, S. Lumped parameter modelling and an introduction to optimization of one-dimensional nonadiabatic drying systems. *Int. J. Heat and Mass Transfer*, 1984, **27**(11), 1971–1983

61 Sieniutycz, S. A development of the relation between drying energy savings and thermodynamic irreversibility. *Chem. Eng. Sci.*, 1984, **39**(12), 1647–1659

62 Van den Bulck, E., Klein, S. A. and Mitchell, J. W. Second law analysis of solid desiccant rotary dehumidifers. ASME Paper No. 85-HT-71, presented at the National Heat Transfer Conference, Denver, Colorado, August 4–7, 1985

63 Lavan, Z., Monnier, J-B., and Worek, W. M. Second law analysis of desiccant cooling systems. *J. Solar Energy Eng.*, 1982, **104**, 229–236

64 Maclaine-cross, I. L. High-performance adiabatic desiccant open-cooling cycles. *J. Solar Energy Eng.*, 1985, **107**, 102–104

65 Moore, B. B. and Wepfer, W. J. Application of second law based design optimization to mass transfer processes. *A.C.S. Symposium Series*, 1983, **235**, 289–306

66 Bejan, A. *Advanced Engineering Thermodynamics*. Wiley, New York, forthcoming